國 立 交 通 大 學

電 信 工 程 學 系 碩 士 班

碩 士 論 文

室內傳環境及天線擺設對多輸入多輸出系統容量之影響分析與量測

Effects of Propagation and Antenna Arrangement on Indoor MIMO Capacity

研究生 ： 張桂福

指導教授 ： 唐震寰 博士

室內傳播環境及天線擺設對多輸入多輸出系統容量之影響分析與量測

Effects of Propagation and Antenna Arrangement on Indoor MIMO Capacity

研 究 生：張桂福　　**Student : Kuei-Fu Chang**

指導教授：唐震寰　　**Advisor : Dr. Jenn-Hwan Tarng**

國 立 交 通 大 學

電 信 工 程 學 系 碩 士 班

碩 士 論 文

A Thesis
Submitted to Institute of Communication Engineering
College of Electrical and Computer Engineering
National Chiao-Tung University
in Partial Fulfillment of the Requirements
for the Degree of
Master of Science
in
Communication Engineering
July 2004
Hsinchu, Taiwan, Republic of China

中 華 民 國 九 十 三 年 七 月

室內傳播環境及天線擺設對多輸入多輸出系統容量之影響分析與量測

研 究 生：張桂福　　指導教授：唐震寰博士

國 立 交 通 大 學

電機資訊學院　　電信工程學系碩士班

摘要

通訊系統為了提高傳輸速率，因而在發射端與接收端使用了多單元天線架構，稱之為多輸入多輸出系統，其系統容量比傳統的一對一天線要來的高。該系統於多路徑環境下利用路徑的低相關性能得到相當高的容量。本論文採用頻域向量通道響應系統模擬八對八及四對四的多輸入多輸出系統，於國立交通大學工程四館內進行量測與分析。對於通道容量而言，吾人發現了下列的幾個現象: (1) 當發射天線單元間距的標準差在一到 1.5 個波長之間，不規則天線架構能比規則天線系統得到較高的通道容量; (2) 系統容量會隨著天線單元間距的增加而增加，但在超過了一個波長之後，天線單元間距對於系統容量就沒有顯著的影響; (3) 系統容量和接收端的擴散角度成正相關;(4) 高的訊號頻寬能得到較大的通道容量;(5) 位於接收端附近的散射體能增加系統的通道容量。

Effects of propagation and Antenna Arrangement on Indoor MIMO Capacity

Student : Kuei-Fu Chang Advisor: Dr. Jenn-Hwan Tarng

Department of Communication Engineering
National Chiao Tung University

Abstract

Multiple-input-multiple-output (MIMO) systems have the potential to achieve very high capacities, depending on the propagation environment. The use of multiple antennas offers extended range and higher throughputs than conventional single antenna communication systems. Large capacity is obtained via the potential decorrelation in the MIMO radio propagation channel since a fully correlated MIMO radio channel only offers one subchannel, while a completely decorrelated MIMO radio channel potentially offers multiple subchannels. The decorrelation effect is dependent on propagation and array arrangement. In this paper, effects of transmitting antenna spacing, multipath angular spreading, signal bandwidth and Tx-Rx distance on the MIMO capacity are investigated through measuremts in indoor environments such as along corridors and classrooms. It is found that (1) When the standard deviation of Tx element spacing is ranging from 1 λ to 1.5 λ, unequally antenna array spacing may have larger capacity than that of the equal spacing; (2)The MIMO capacity increases as the array element spacing increases and it saturates when the spacing is larger than one wavelength. This reveals that the correlation distance between the elements in indoor environments is about one wavelength; (3) Capacity is increased when the propagation distance decreases, or when rms angle spread

increases, or when number of received paths increases. (4) Higher signal bandwidth obtains higher capacity, since more multipath components are resolved, which leads to less spatial correlation.

誌謝

首先，我要對我的指導教授唐震寰老師致上最誠摯的感謝，感謝老師在我碩士兩年的研究生涯中，給于我最細心與凡心的指導與叮嚀，並帶領我一窺無線通訊領域研究的奧妙。

其次，對於波散射與傳播實驗室的學長與同學們也要致上我深深的謝意，他們所給予我在知識上和精神上的啟示與鼓勵以及在實驗量測中的協助，對完成本篇論文有莫大的助益。

最後，要感謝的是我的家人，由於他們給予我的支持與關懷，使我在人生的過程裡得到最細心的呵護與照顧，讓我在成長與求學的過程中能夠有所依靠。

僅以此篇論文獻給所有關心我的人。

張桂福

國立交通大學，新竹市

中華民國九十三年七月

Contents

List of Figures

List of Tables

Chapter 1

Introduction

Multiple-Input Multiple-Output (MIMO) communications systems using multi-antenna arrays simultaneously during transmission and reception have generated significant interest in recent years. Multiple antenna technologies are being considered as a viable solution for the next generation of mobile and wireless local area networks (WLAN). The use of multiple antennas offers extended range, improved reliability and higher throughputs than conventional single antenna communication systems. MIMO systems also have emerged as one of the most promising approaches for high-data rate wireless systems, MIMO communication architecture which employs multiple antennas at both the transmitter and the receiver, has recently emerged as a new paradigm of extremely spectrum-efficient wireless communications in rich multipath environment. MIMO wireless systems have been shown theoretically to have significantly higher capacity than more traditional single-input multiple-output (SIMO) systems. Large capacity is obtained via the potential decorrelation between the channel coefficient of the multiple-input/multiple-output (MIMO) radio channel, since a fully correlated MIMO radio channel only offers one subchannel, while a completely decorrelated radio channel potentially offers multiple subchannels depending on the antenna configuration and propagation effects. Increase in the correlation coefficient results in capacity decrease and, finally, when the correlation coefficient equals to unity, no advantage is provided by the MIMO architecture.

In the MIMO systems, for a completely uncorrelated channel matrix, the MIMO capacity reaches its maximum and scales roughly linearly as the number of antennas. The capacity of MIMO systems has been shown to increase linearly with the number of antennas

in an ideal i.i.d. channel [1],[2]. Thus to investigate effects of propagation and array arrangement on the correlation of the channel matrix, which will affect MIMO capacity, will be an interesting and important subject. The effect of antenna spacing is reported in reference [3] that the antenna spacing has little effect on capacity when the antenna spacing exceeds 0.5 wavelength, However, our measurement results and the result shown in reference [3] found that the antenna spacing actually affects significantly. In the reference [3], it show that when the antenna array spacing exceed 0.5wavelength , the capacity will increase very slowly, but according to our research , we find that when antenna array spacing exceed one wavelength，capacity will saturation，but between 0.1 wavelength to the 1 wavelength , the capacity will linearly increase when antenna array spacing increase. In most of the paper, the antenna array spacing is equal, but we find that the unequally array spacing maybe obtains the greater capacity than the equal array, in the reference [4], we can observe the same result. In other literatures, the distance between the transmitter and receiver not analyzes in detail. In this thesis we will also investigate the capacity versus distance between the transmitter and the receiver, and compare the result with reference [5]. In the reference [6] and [7], capacity of uncorrelated channel is greater than correlated channel and large antenna spacing has lower correlation coefficients. We also obtain the same result according to our measured data. The above mentioned works are summarized in Table I.

In this thesis, we will introduce the correlation properties of MIMO channels and analyze the measured indoor MIMO channel data to investigate the effects of antenna spacing, multipath, angle spread and Tx-Rx distance. We also compare the capacity of equal antenna array spacing and unequal antenna array spacing.

In our research, effects of transmitting antenna spacing, multipath angular spreading and Tx-Rx distance on the MIMO capacity are investigated through measure in indoor

environments such as along corridors. It is found that (1) Most unequally antenna array spacing cases have larger capacity than that of equal spacing; (2) Capacity is highly correlated with the neighboring elements spacing. However, this phenomenon is not so obvious when the spacing is larger than one wavelength; (3) Capacity is increased when the propagation distance decreases, or when angle spread increases,

or when number of received paths increases.

This thesis is composed of 5 chapters as following: In chapter 2, the fundamental theory of MIMO systems will be introduced. The general Shannon capacity formula is used to compare the capacity performance of MIMO systems . Chapter 3 is the MIMO channels measurement in the hallway. We will describe the MIMO channels measurement system and the measurement sites. In chapter 4, according to the measured data , the capacity and correlation coefficients of MIMO channel will be defined and calculated. The effects of antenna spacing, angle spread, equally antenna array and unequally antenna array, and Tx-Rx distance at both ends will be considered. A brief conclusion is provided in Chapter 5.

Table 1. Review of related result

Ref. No.	Freq. (GHz)	Measurement Environment	Related Measurement Result
[3]	5.1-5.3	1. entrance hall 2.Tx and Rx are 10m apart	The capacity will increase slowly when the antenna element spacing exceed 0.5 wavelength
[4]	5.8	Indoor environment (virtual transmitter antenna and receiver antenna array)	Unequal array spacing may obtain the optimum capacity
[5]	1.95	Along hallway, Tx-Rx distance 270ft	Capacity decreases with distance increases
[6]	2.4	1.Indoor environment 2.2×2 MIMO system	Capacity of uncorrelated channel is greater than correlated channel
[7]	0.6-6	1.Indoor environment 2.2×2, 4×4, 10×10 MIMO systems	Large antenna spacing has lower correlation coefficients

Chapter 2

MIMO Systems

Multiple-input multiple-output (MIMO) wireless systems have been shown to be a very promising solution for high data rate and/or high performance future wireless networks and services. It was demonstrated that, by means of receive diversity, the impairment due to a rich scattering environment could be actually exploited to obtain independent fading signals, thus enhancing the quality of the received signal by means of optimum combining [8]. On the other hand when multiple antennas are employed at both sides of the communication link, it was shown that, in presence of a rich multipath, there is considerable potential for obtaining extremely high capacities.

In this chapter we will introduce fundamental theory of MIMO system and compare single-input-single-output (SISO), single-input-multiple-output (SIMO), and MIMO capacities.

2.1 Why Use MIMO?

There are many reasons making MIMO systems such a promising solution for future wireless communications. As it will be shown the main advantage is given by the huge capacity/spectral efficiency these systems can achieve, thanks to the multiple spatial subchannels opened through the use of multiple transmit and receive antennas. It is not the only one though, another important characteristic is the higher diversity order that can be reached by means of multiple independent replicas of the transmitted signal, and some more advantages exit.

2.2 MIMO Architecture

Consider the MIMO setup pictured in Fig.2-1 with M antennas at the BS and N antennas at the MS. The signals at the BS antenna array are denoted by the vector $y(t) = [y_1(t), y_2(t), ..., y_M(t)]^T$, where $y_m(t)$ is the signal at the mth antenna port and $[\cdot]^T$ denotes transposition. Similarly, the signals at the MS are $S(t) = [s_1(t), s_2(t), ..., s_n(t)]^T$.

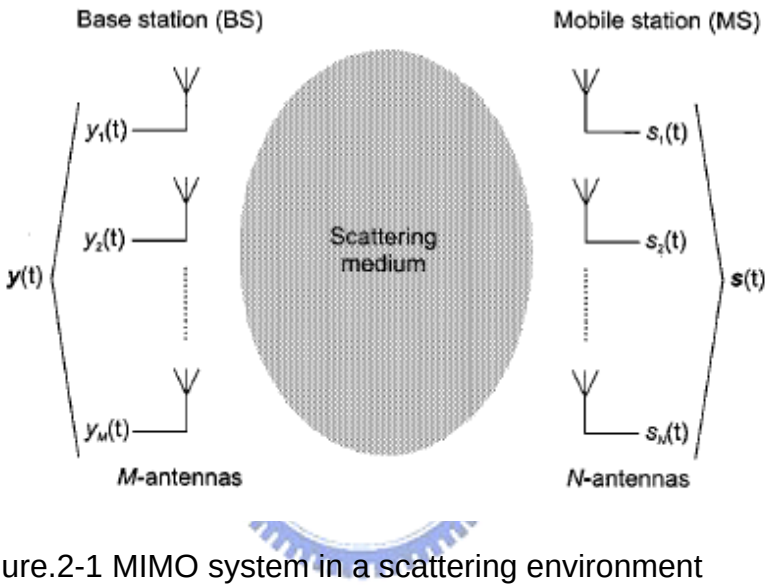

Figure.2-1 MIMO system in a scattering environment

The MIMO radio channel $H \in C^{M \times N}$ that describes the connection between the MS and BS can be expressed as

$$H = \begin{pmatrix} h_{11} & h_{12} \cdots & h_{1N} \\ h_{21} & \ddots & \vdots \\ \vdots & & \\ h_{M1} & h_{M2} \cdots & h_{MN} \end{pmatrix}$$

where h_{mn} is the complex transmission coefficient from antenna n ate the MS to antenna m at the BS. For simplicity, it is assumed that h_{mn} is complex Gaussian distributed with

identical average power. Thus, the relation between the vectors y(t) and s(t) can be expressed as $y(t)=H(t)s(t)+n(t)$

$$\begin{bmatrix} y_1 \\ y_2 \\ \vdots \\ y_M \end{bmatrix} = \begin{pmatrix} h_{11} & \cdots & h_{1N} \\ \vdots & \ddots & \vdots \\ h_{M1} & \cdots & h_{MN} \end{pmatrix} \begin{bmatrix} s_1 \\ s_2 \\ \vdots \\ s_N \end{bmatrix} + \begin{bmatrix} n_1 \\ n_2 \\ \vdots \\ n_M \end{bmatrix}$$

where n is zero-mean complex Gaussian noise.

From Shannon formula we can obtain the MIMO capacity can be express as

$$C = \log_2(\det\{I_{N_R} + \frac{\rho}{N_T} HH^H\}) \quad \textbf{(bps/Hz)}$$

where N_T and N_R are the number of Tx and RX antenna array elements, respectively, and I_{N_R} is N_R-by-N_R identity matrix, H is the N_R-by-N_T channel transfer matrix with its element h_{ij} representing the channel gain between j-th Tx and I-th Rx, and the superscript "H" means transpose and conjugate. If in the frequency domain the formula becomes :

$$C(f) = \log_2(\det(I_8 + \frac{\rho}{8} H(f)H(f)^H)) \text{ .....(2-1)}$$

Note that the channel matrix H is normalized to remove the path and yields [8]:

$$\sum_{i,j} |h_{ij}|^2 = n_T$$

2.3 Spatial Correlation Coefficient

The complex correlation coefficient is a complex number that is less than unity in absolute value. Let a,b be two complex random variables. The complex correlation coefficient of a and b is defined as

$$< a,b >= \frac{E[ab^*] - E[a]E[b^*]}{\sqrt{\left(E\left[|a|^2 - |E[a]|^2\right]\right)\left(E|b|^2 - |E[b]|^2\right)}} \quad \text{.....(2-2)}$$

Where * denotes the complex conjugate operation. It is assumed that all antenna elements in the two arrays have the same polarization and the same radiation pattern. The spatial complex correlation coefficient at the BS between antenna m_1 and m_2 is given by

$$\rho_{m_1 m_2}^{BS} = < h_{m_1 n}, h_{m_2 n} >$$

where <a, b> computes the correlation coefficient between a and b. The spatial complex correlation coefficient observed at the MS is similarly defined as

$$\rho_{m_1 m_2}^{MS} = < h_{m n_1}, h_{m n_2} >$$

Given (2-2-1) and (2-2-2), one can define the following symmetrical complex correlation Matrices

$$R_{BS} = \begin{pmatrix} \rho_{11}^{BS} & \rho_{12}^{BS} \cdots & \rho_{1M}^{BS} \\ \vdots & \ddots & \vdots \\ \rho_{M1}^{BS} & \rho_{M2}^{BS} \cdots & \rho_{MM}^{BS} \end{pmatrix}_{M \times M}$$

and

$$R_{MS} = \begin{pmatrix} \rho_{11}^{MS} & \rho_{12}^{MS} \cdots & \rho_{1N}^{MS} \\ \vdots & \ddots & \vdots \\ \rho_{N1}^{MS} & \rho_{N2}^{MS} \cdots & \rho_{NN}^{MS} \end{pmatrix}_{N \times N}$$

$$\rho^{BS} = \frac{1}{M(M-1)} \left(\sum_{\substack{i=1, j=1 \\ i \neq j}}^{M} \left| \rho_{m_i m_j}^{BS} \right| \right) \quad \text{.....} \quad (2\text{-}3)$$

$$\rho^{MS} = \frac{1}{N(N-1)} \left(\sum_{\substack{i=1, j=1 \\ i \neq j}}^{N} \left| \rho_{n_i n_j}^{MS} \right| \right)$$

Receiver correlation describes the local scattering around the receivers, whereas transmitter correlation describes the correlation of the transmitted signals as seen at the receiver and does not provide insight into the scattering of the environment close to the transmitter array.

2.4 Capacity Formulas Of Four Different System

A. Single-Input-Single-Output (SISO) system

For a 1*1 (SISO) system the capacity is given by

$$C = \log_2(1 + \rho \left| H \right|^2) \quad \textbf{(bps/Hz)}$$

Figure 2-2 SISO system

where **C** is the capacity, ρ is the signal-to-noise ratio (SNR) and **H** is the normalized channel power transfer function. For 1-D case **H** is simply a complex scalar. The capacity increases slowly with $\log_2$(SNR).

B. Single-Input-Multiple-Output (SIMO) system

For a SIMO system the capacity is given by

$$C = \log_2(1 + M * \rho) \quad \textbf{(bps/Hz)} \qquad (2\text{-}5)$$

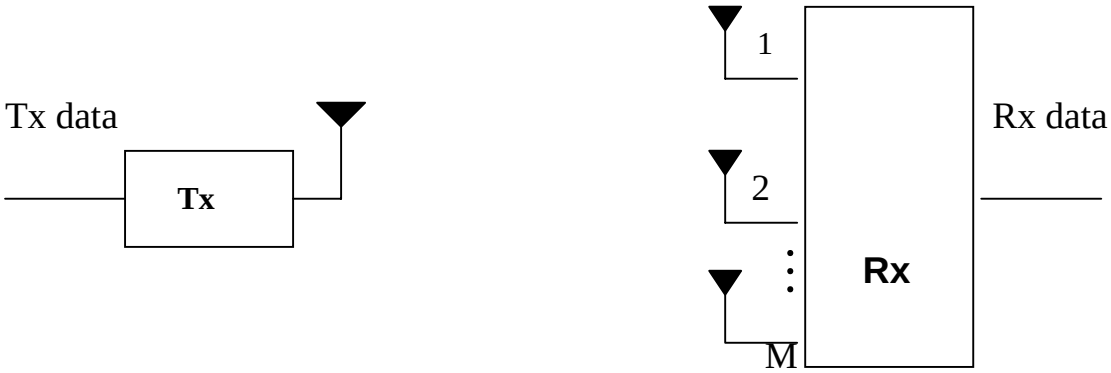

Figure 2-3 SIMO system

Compared with SISO system, the capacity of SIMO system shows improvement. The increase in capacity is due to the spatial diversity, which reduces fading and SNR improvement. However, the SNR improvement is limited, since the SNR is increasing inside the log function.

C. Multiple-Input-Single-Output (MISO) system

For a MISO system the capacity is given by

$$C = \log_2(1 + \frac{\rho}{N}\sum_{n=1}^{N}|h_n|^2) \quad \textbf{(bps/Hz)}$$

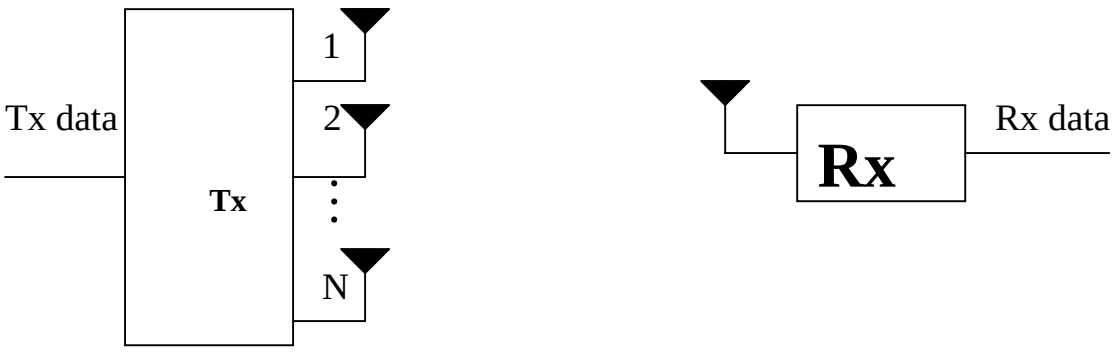

Figure 2-4 MISO system

D. Multiple-Input-Multiple-Output (MIMO) system

For a MIMO system with N_T transmit and N_R receive antennas, it is shown that the capacity is derived from

$$C = \log_2(\det\{I_{N_R} + \frac{\rho}{N_T} HH^H\}) \quad \textbf{(bps/Hz)}$$

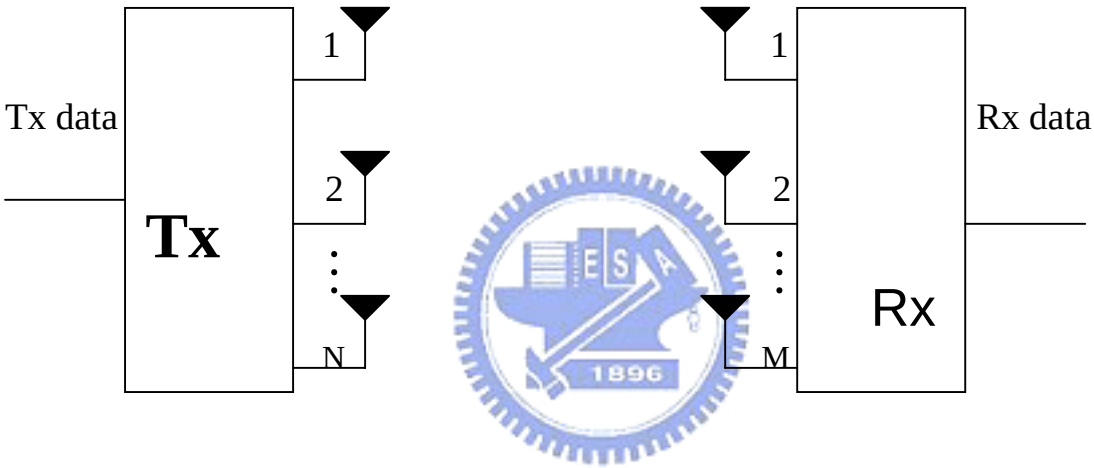

Figure 2-5 MIMO system

Here , we can see that the advantage of MIMO systems is significant in capacity. As an example, for a large $N_T=N_R=N$, $HH^H/N \rightarrow I_N$, so the capacity is asymptotic to

$$C \approx N\log_2(1+SNR)[bps/Hz]$$

Therefore, the capacity increases linearly with the number of transmit antennas. Figure 2-6 shows the capacity for various multiple antennas systems. It is show that SIMO systems offer smaller capacity gain than MIMO systems. For example, MIMO system with $N_T=N_R=2$ provides higher capacity than SIMO system with $N_T=1$ and $N_R=4$ [3]

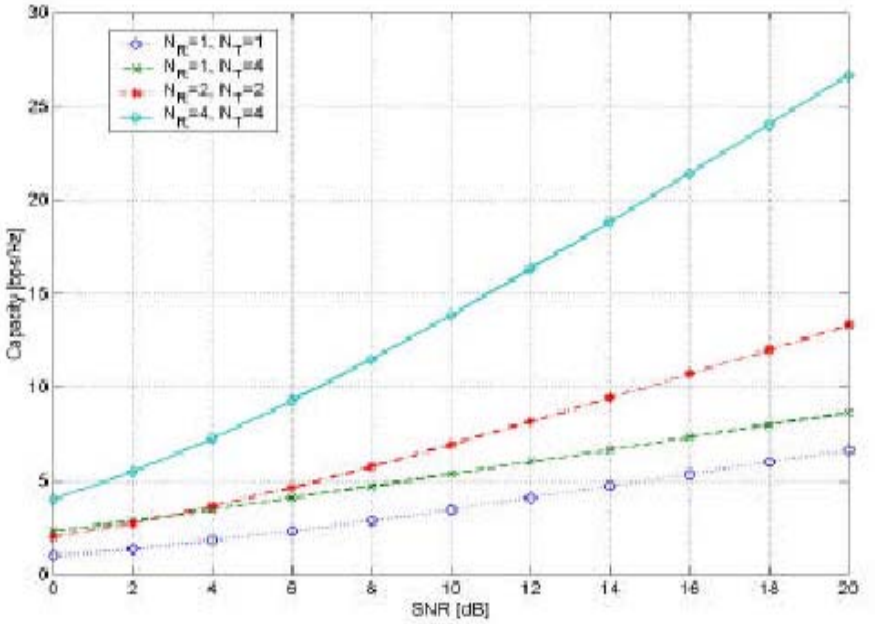

Figure.2-6 Capacity comparison of several multiple antenna systems

Chapter 3

Measurement System and Environment

MIMO radio channel access based on dual antenna arrays at both the mobile station (MS) as well as base station (BS) is considered to be the ultimate means to increase the available capacity for high bit rate wireless links. By this technique the spatial diversity of multipath channels in a rich scattering environment is optimally exploited. Several results have been published showing the MIMO capacity gain in theory (e.g.[1],[10]). Some results were based on virtual array application and hence a static channel had to be presumed.

In this chapter we will describe the measurement systems and the measurement sites.

3.1 Measurement Systems

For measurement of the time-varying and directional mobile channels, RUSK vector channel sounder is employed [9], whose system diagram and equipment are shown in figures 3-1 and 3-2. The sounder system consists of a mobile transmitter (Tx) that is omni-directional, and a fixed receiver (Rx) with an 8-element array antenna. Periodic multi-frequency excitation with 120MHz bandwidth is used, i.e., the time resolution is 8.3ns. The Doppler bandwidth of up to 20kHz allows complete statistical analysis of the time varying radio channel with respect to different azimuthally directions of the

impinging waves. In the case of a remote link measurement, Tx/Rx synchronization is maintained the tracking error of the measurement system and as a result of phase and delay normalization. Allowing the system a warm-up time about 60 minutes to stabilize oscillator amplifier minimizes temporal drift of the measurement system. The telemetry allows remote of the digital receiving unit (DRU) from portable transmitting station (PTS) location. The device operates at 2.44 GHz and permits real-time measurements of the complex channel impulse response with a bandwidth of 120 MHz. The measurement principle is based on periodic multi-frequency excitation signals, the recorded signal vector consists of integer periods of the received excitation signal response, it can be transformed to the frequency domain by FFT processing. Then , the measurement results can be directly interpreted as a time-dependent sequence of the channel frequency response estimates. The data is captured by simultaneous multiplexing of the receive antennas employing fast RF switches. Thereby rubidium reference oscillators at both transmitter and receiver achieve timing and switching frame synchronization between receiver and transmitter during the complete measurement.

The channel impulse responses of the antenna array are recorded as “vector snapshots” in rapid succession. After receiving by Rx, signals are gathered to DRU and sent to a personal computer(PC) to analyze by using Unitary ESPRIT with sub-array smoothing technology. An overview about array signals processing including estimation of the AOA and a comparison of ESPRIT with other algorithm can be found in [10].

3.2 Measurement Setup

For the measurements, we used the wideband vector channel sounder RUSK ATM with a measurement bandwidth of 120 MHz at a center frequency of 2.44 GHz. At the receive side a $\lambda/2$ spaced 8-element uniform linear patch array (ULA) with two

additional dummy elements was used. Each single patch antenna had a 3dB beamwidth of 120 degree and was consecutively multiplexed a single receiver chain. At the transmit side, a omni-directional antenna was moved along the measured path, we can form 8 virtual Tx antenna array without mutual coupling.

The receiving antenna was mounted on a rooftop at 2.44GHz with the transmission power of 1W. The transmitter antenna was carried in a trolley and was 1.8 meter above the road. In order to get multipath components, we sampled data by fixed-point and moving measurements along selected routes with walking speed

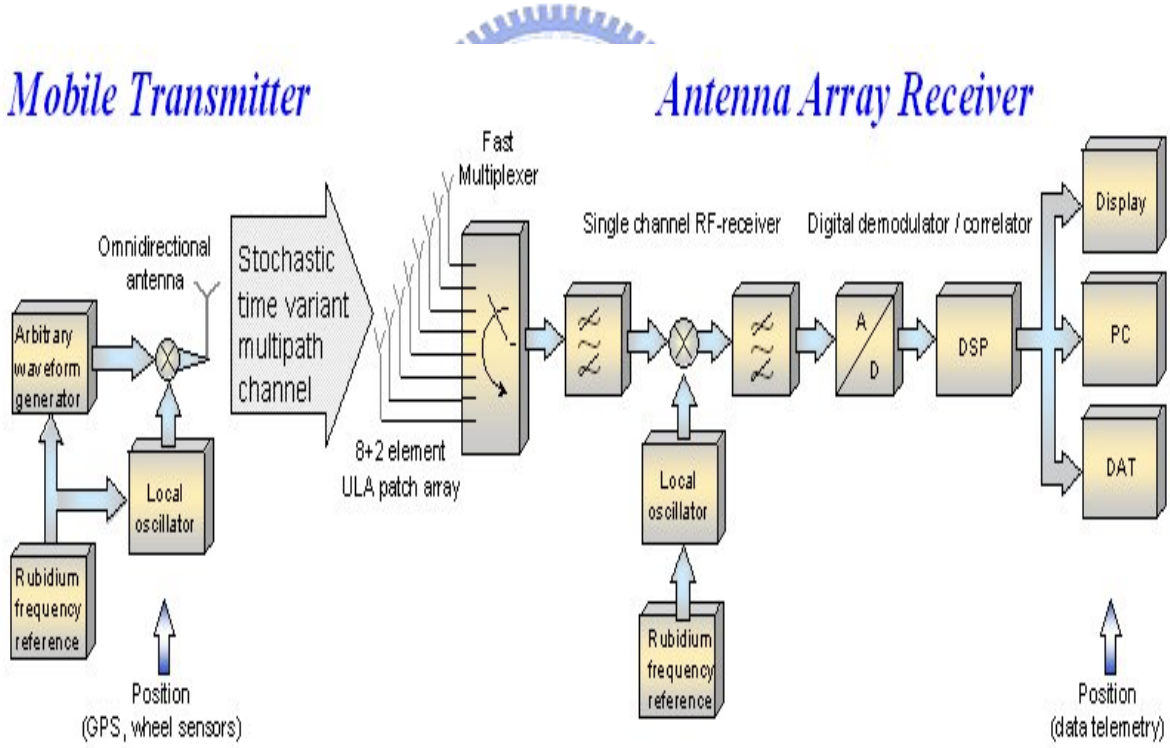

Figure 3-1 System diagram of the RUSK Channel Sounder

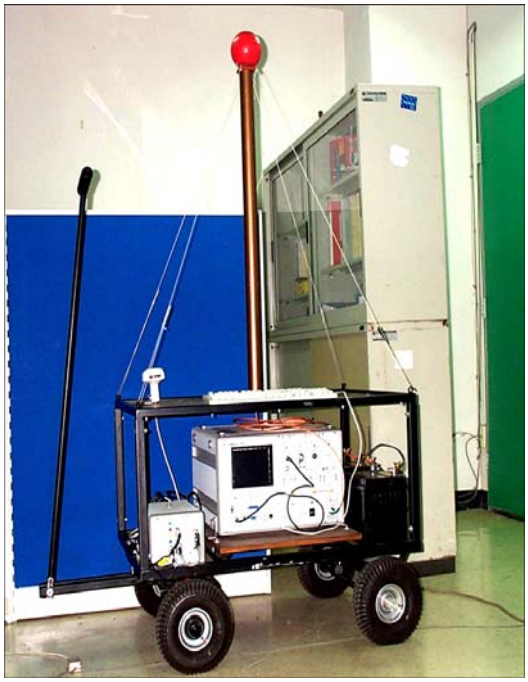

Figure 3-2 pictures of the RUSK Channel Sounder (a) transmitter with an omnidirectional antenna; and (b) the receiver with 8-element linear antenna

3.3 Measurement Environment Description

The measurement was performed in 9th floor (site A), 2nd floor (site B), 3st floor (site C), 4st floor (site D) and 5st floor (site E) of the 4th Engineering Building at the National Chiao-Tung University, Hsinchu, Taiwan and the layout is shown in Figs. 3-3 to 3-6.

At site A, path 1 and path2 is measured in the corridor, thus LOS always exists in path 1, instead LOS, the NLOS exists in path 2.At site B path1 is the LOS environment and the distance is longer than the site A, we will observe how the long distance affect the capacity.

Site D and site E is measured also in the hallway, but at the site E, the wall is constructed of the glasses and at site D is concrete wall. We will explore the different material how to affect the capacity.

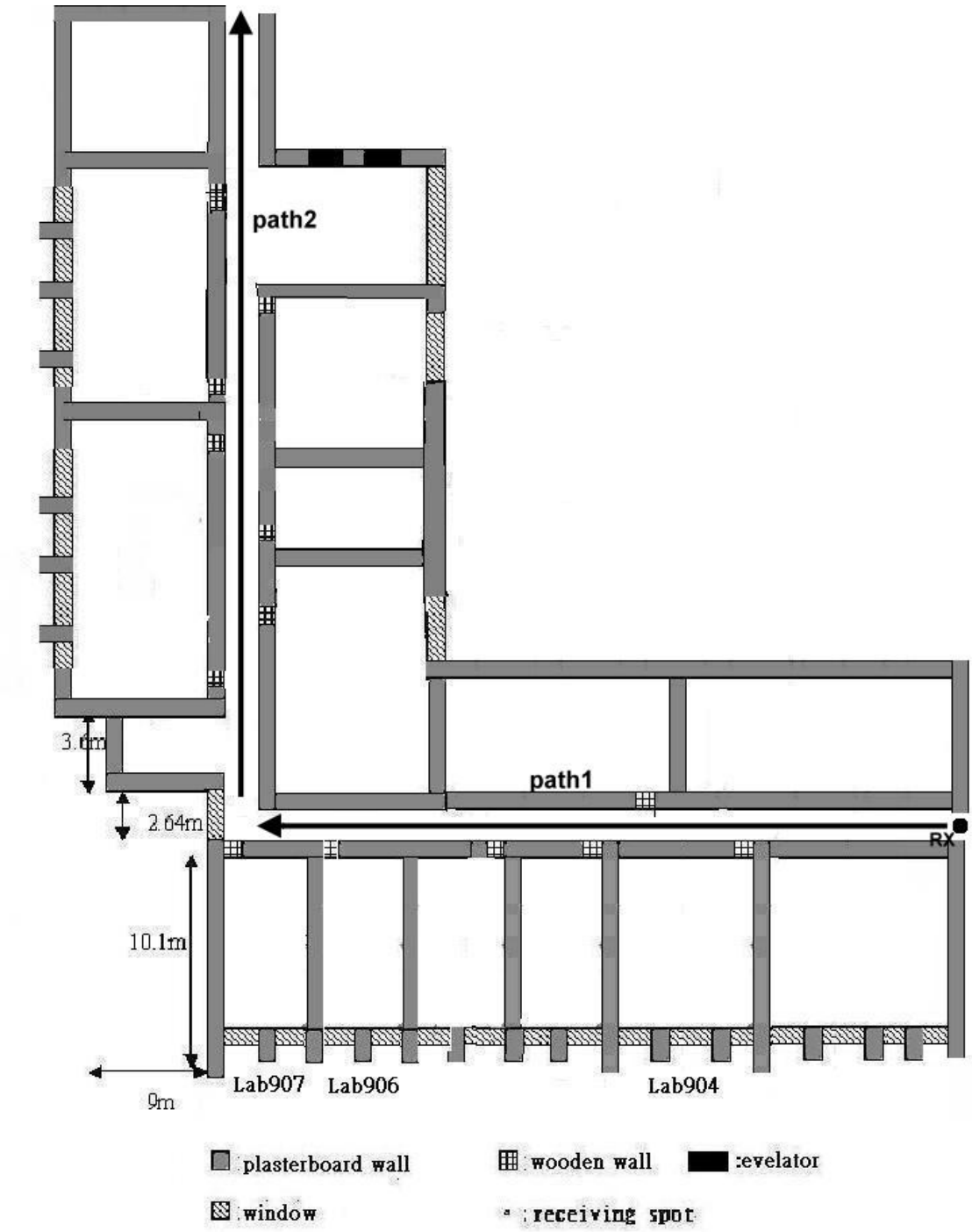

Figure 3-3 Floor layout of site A located on the second floor of Engineering Building No4

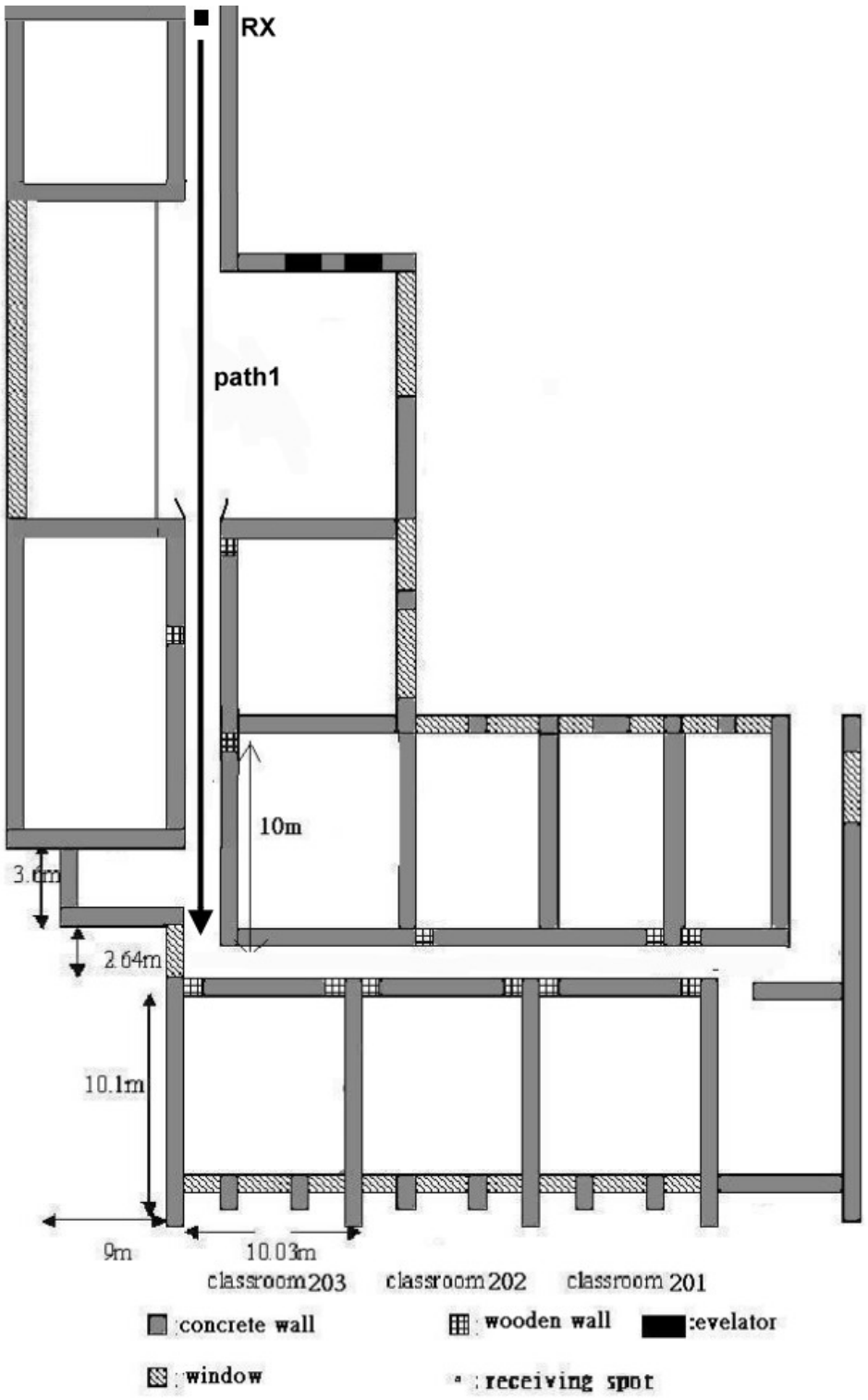

Figure 3-4 Floor layout of site B located on the second floor of Engineering Building No4

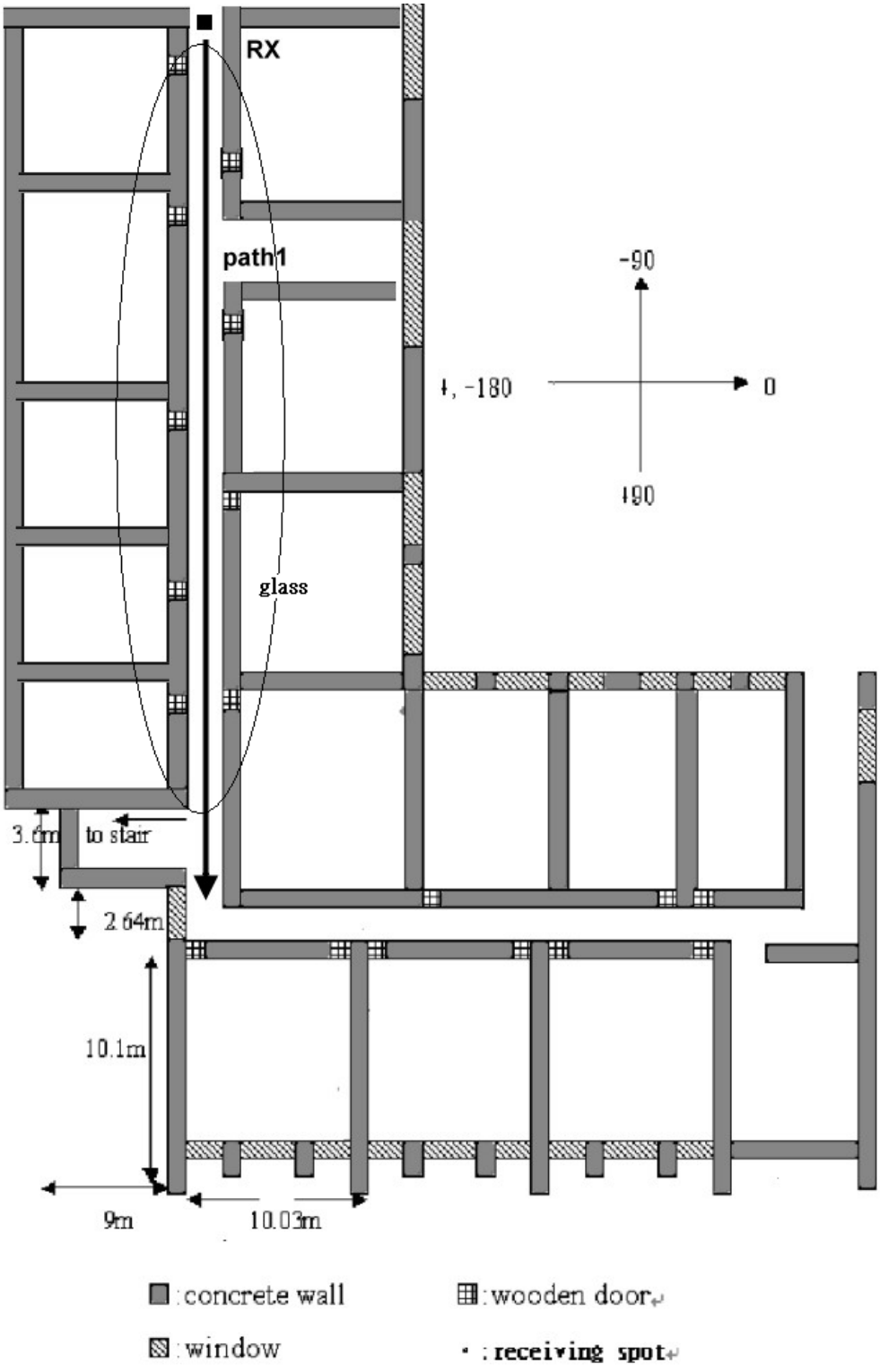

Figure 3-5 Floor layout of site C located on the second floor of Engineering Building No4

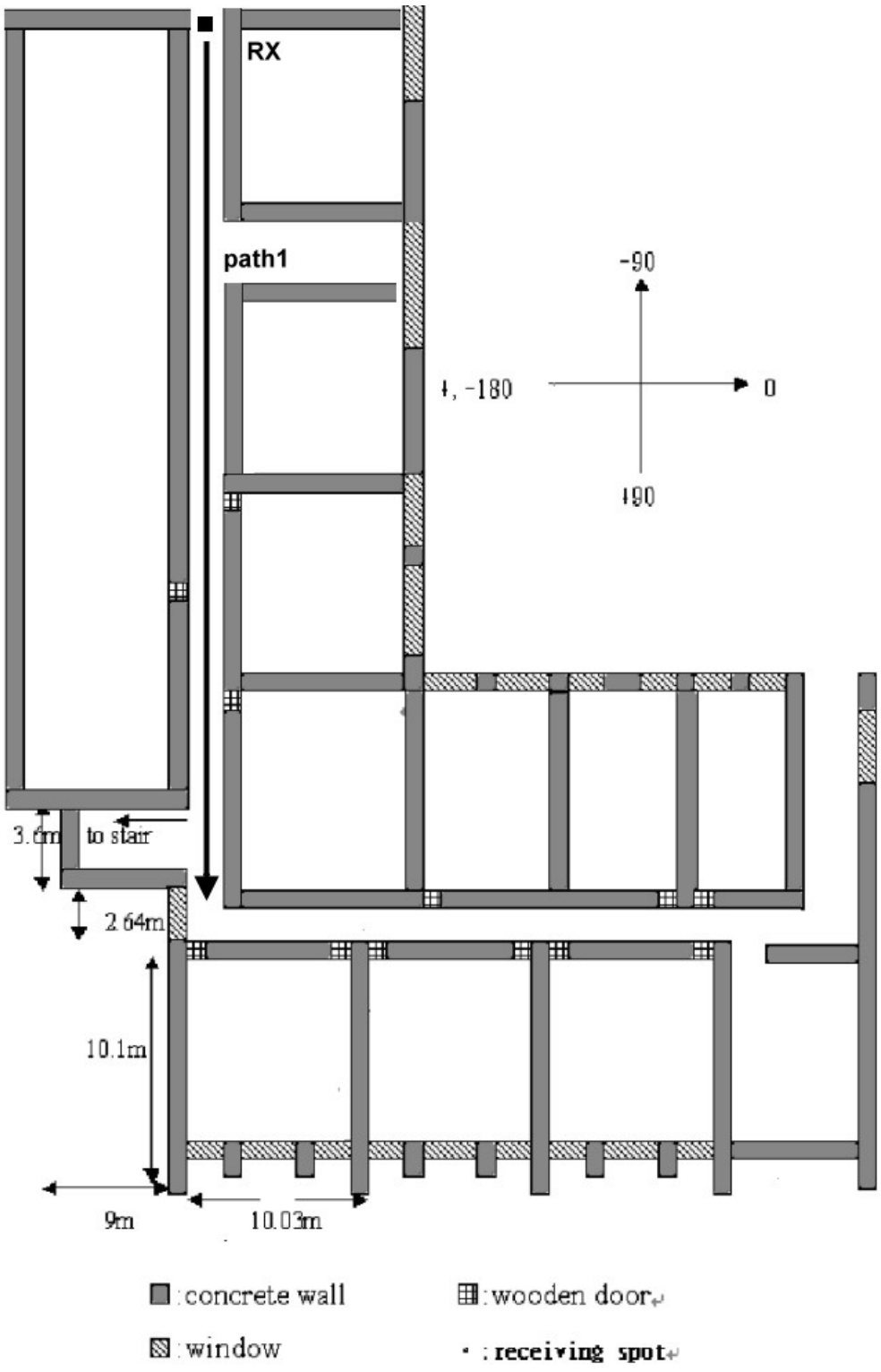

Figure 3-6 Floor layout of site D located on the second floor of Engineering Building No4

Table 2 Measurement situation

hallway		Frequency	Power	Bandwidth	Sample point	Distance(m)
Site A	Path1	2.44GHz	1 W	120 MHz	21900	24
	Path2	2.44GHz	1 W	120 MHz	43000	53
Site B	Path1	2.44GHz	1 W	120 MHz	26550	42
Site C	Path1	2.44GHz	1 W	120 MHz	22100	48
Site D	Path1	2.44GHz	1 W	120 MHz	23500	48

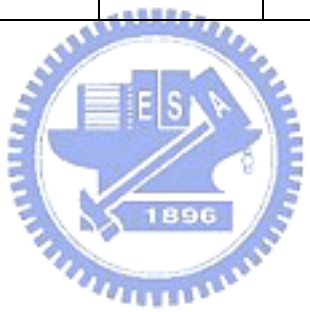

Chapter 4

Effects of Array Element Spacing and Multipath Propagation on MIMO Capacity in Indoors

In this chapter, the effects of transmitting/receiving array spacing, propagation conditions (LOS and NLOS), and local scatterer distribution and signal bandwidth on MIMO capacity are investigated through the measurement. The complex correlation coefficients of the MIMO channel frequency response will be introduced and evaluated.

4.1 MIMO capacity evaluation

From Eq. (2-1), the 8x8 MIMO capacity is given by

$$C(f) = \log_2(\det(I_8 + \frac{\gamma}{8} H(f) H(f)^H))$$

The capacity is calculated with γ =30 dB and the measured 8x8 MIMO channel matrix, H, which is realized through the measurement by the RUSK channel sounder systems. During the measurement, a virtual 8-element linear array at transmitting site is formed by grouping 8 associated Tx positions with chosen neighboring-position spacing.

From equation (2-3), the spatial correlation coefficient at the transmitter between elements is calculated.

4.2. Propagation distance and array-element spacing effects

To investigate propagation and the element spacing effects on the MIMO capacity and Tx-Rx element correlation, the measurement routes have been selected to consider LOS and NLOS scenarios at Site A.

A. Propagation range effect

Figures 4-1 and 4-2 illustrate the MIMO capacity versus Tx-Rx distance for LOS and NLOS scenarios, respectively. In each figure, the array element spacing, Δ, is equal to 0.1 λ, 0.2 λ,…., or 1.0 λ. The figures show that the capacity is decreased as the Tx-Rx distance increases for both LOS and NLOS cases. It is because that when the Tx-Rx distance decreases, the rms angle spread of AOA increases, which reduces the correlation between the Tx and Rx elements, i.e., enhances the capacity. In the next section, we will analyze the relation of angle spread and MIMO capacity. Figures 4-3 and 4-4 show the correlation coefficient versus propagation distance for LOS and NLOS scenarios, respectively. The spatial correlation coefficient increases as the Tx-Rx distance increases.

B. Element spacing effect

From figures 4-1 to 4-4, it is also found that larger element spacing leads to lower correlation coefficient, i.e., higher MIMO capacity.

To further investigate the effect of element spacing, figures 4-5 and 4-6 illustrate capacity versus element spacing for LOS and NLOS scenarios, respectively. It is found that the capacity increases as the element spacing increases and it saturates when the spacing is larger than one wavelength. This reveals that the correlation distance between the elements in indoor environments is about one wavelength.

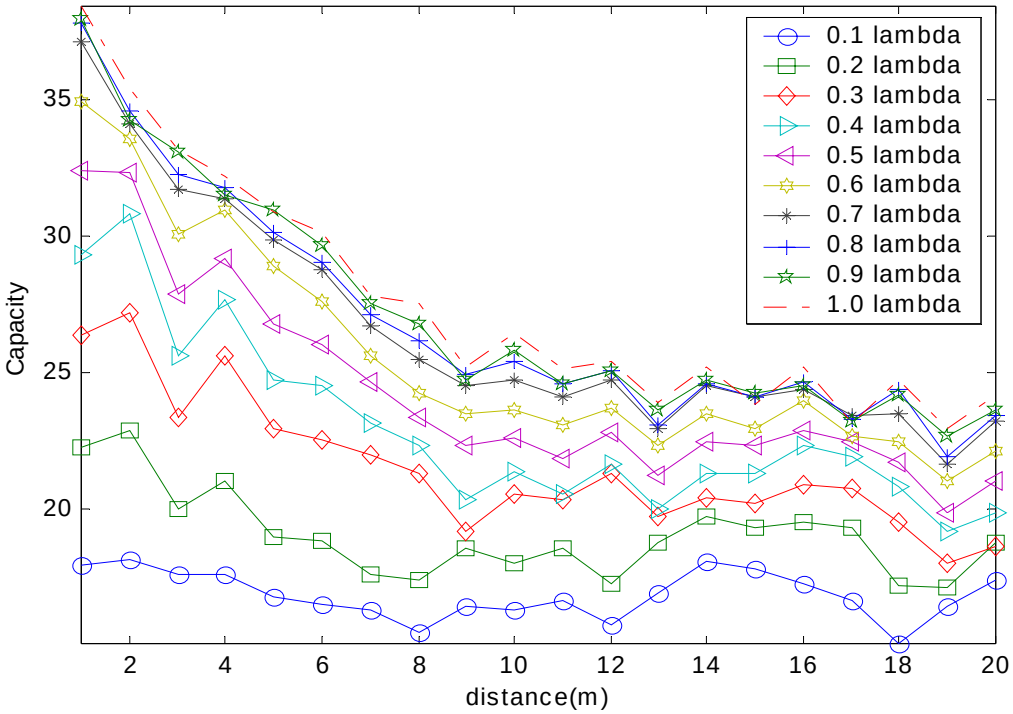

Figure 4-1 Capacity versus Tx-Rx distance (d) for different Tx element spacing (LOS)

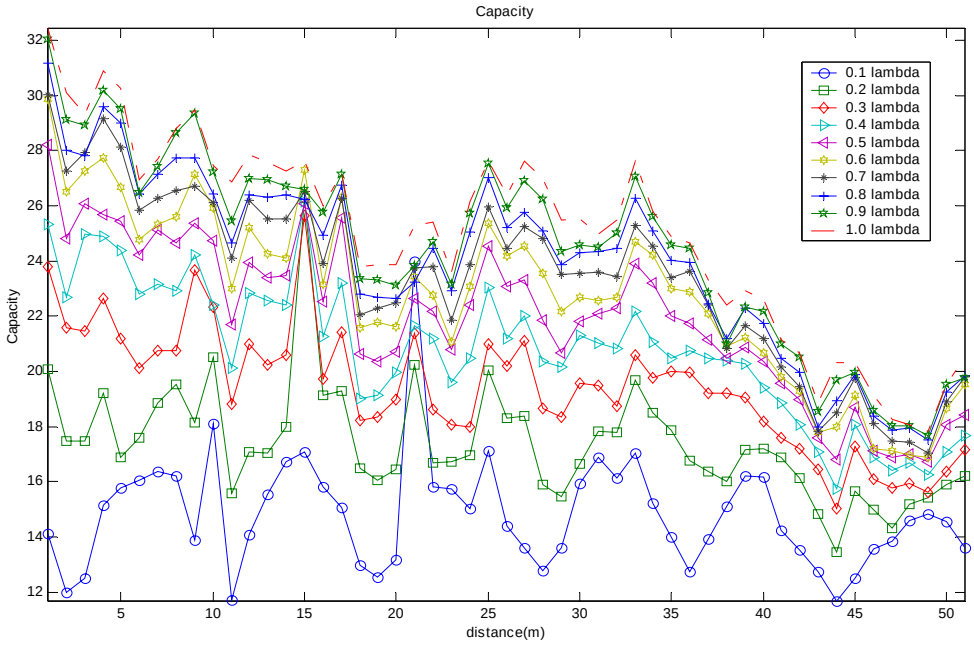

Figure 4-1 Capacity versus Tx-Rx distance (d) for different Tx element spacing (NLOS)

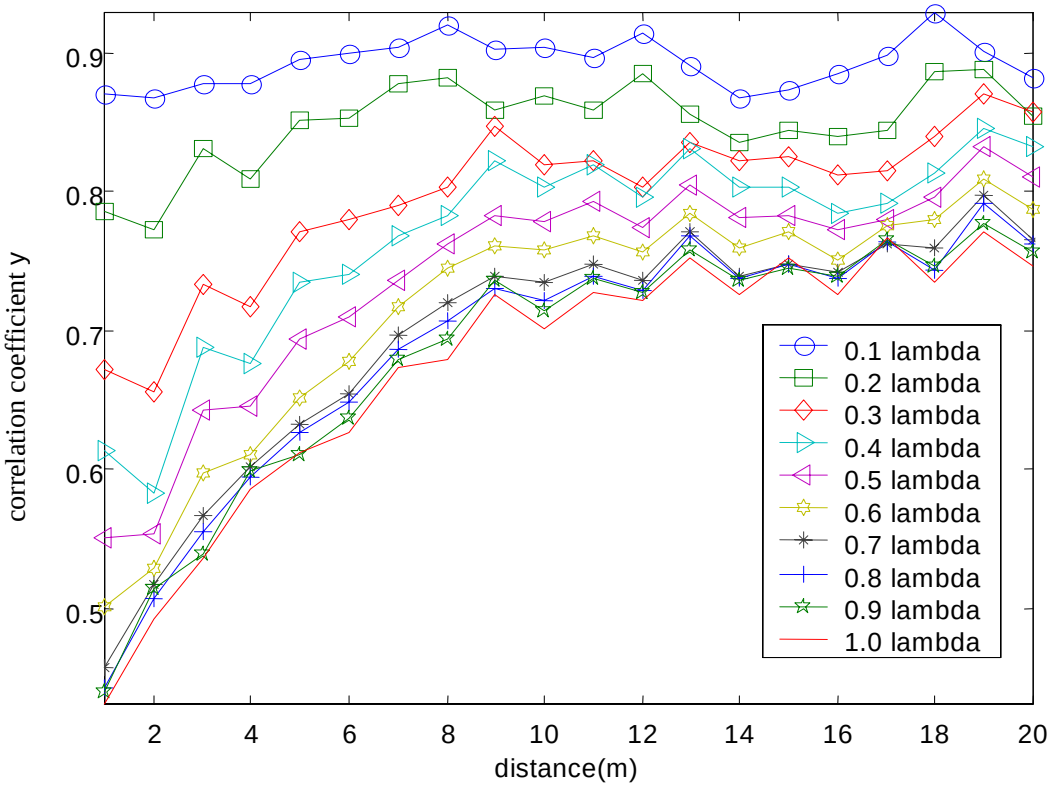

Figure 4-3 Correlation coefficient versus d for different Tx element spacing (LOS)

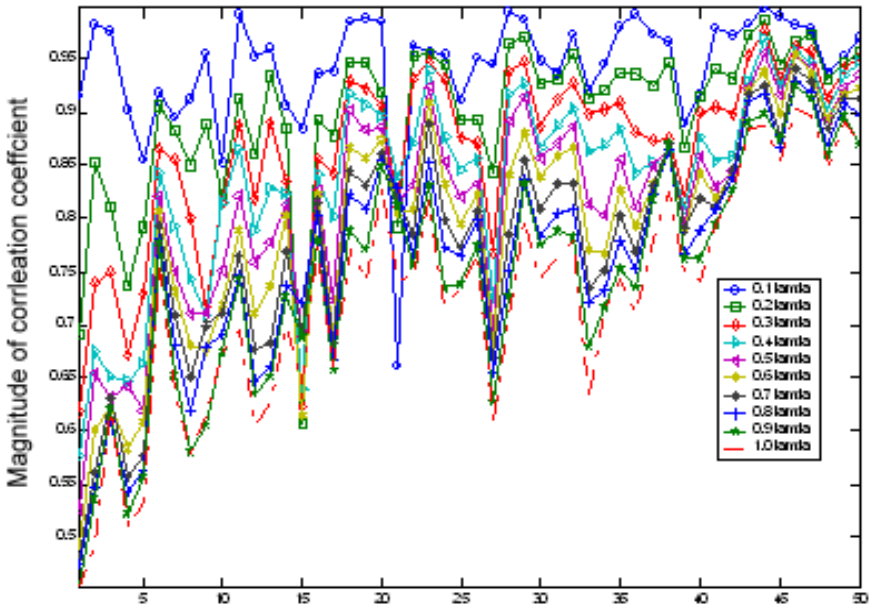

Figure 4-3 Correlation coefficient versus d for different Tx element spacing (NLOS)

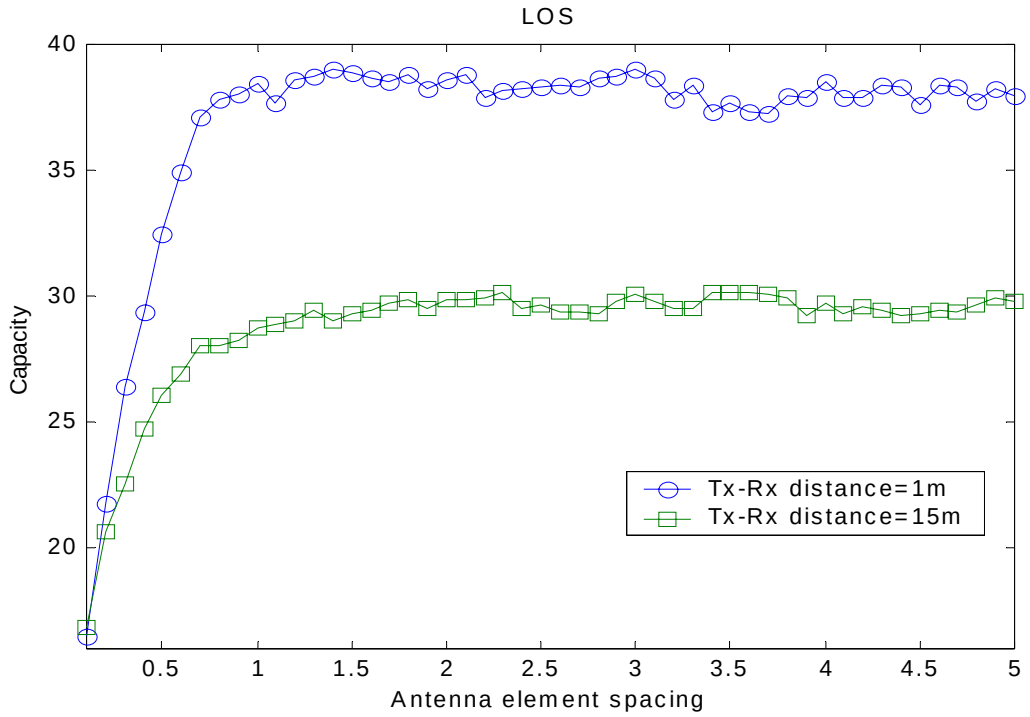

Figure 4-5 Capacity versus transmitter antenna element spacing for LOS

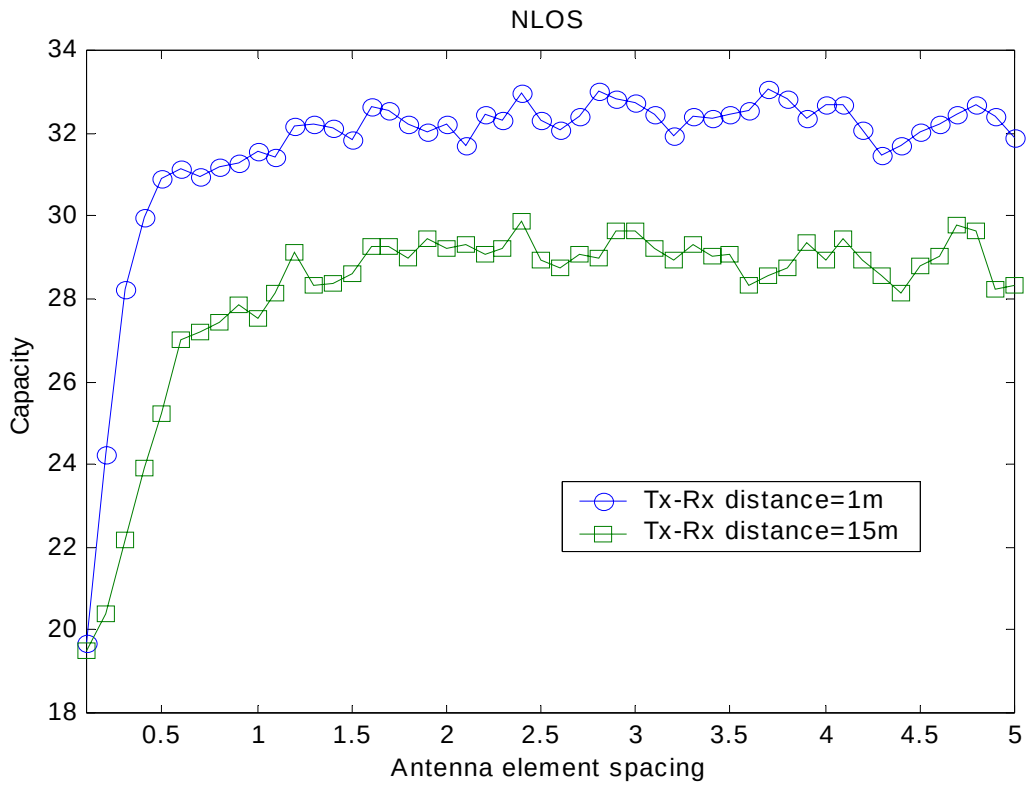

Figure 4-6 Capacity versus transmitter antenna element spacing for NLOS

C. Effect of unequal element spacing

In the MIMO system, channel capacity may be improved by adaptively changing the element spacing. Changing the element spacing is a way to provide spatial diversity to a MIMO link without increasing the number of antenna array elements [4]. In this thesis, we consider adapting the location of elements at both ends of the link. Here, we adjust the element spacing of the virtual antenna arrays at the transmitter to investigate how the capacity varies with small changes in element locations.

To investigate how the channel capacity changes with element spacing, and how much benefit we can get by the adaptive array. From measured data of site A, we synthesized virtual 141-element uniform linear arrays, whose neighboring element spacing is 0.1λ. At the receiver the number of antenna arrays is fixed to 8 and the antenna array spacing is 0.4λ (Following the RUSK sounder specification). The channel matrices of unequally spaced array elements can be determined as subsets of the measured (141,8) MIMO channel. We randomly choose 8 element at transmitter to form an 8×8 MIMO without mutual coupling. Figures 4-7 and 4-8 demonstrate MIMO capacities of unequal- and equal- spacing arrays for LOS and NLOS cases, respectively. The element spacing of the equally spaced array is equal to 2λ. The figures show that the unequal spacing arrays always lead to an optimum capacity, which is better than that of the equal spacing arrays.

The reference [4] mentioned that if both transmitter antenna array spacing and receiver antenna array spacing is unequal; the capacity will reach the maximum. Now we also change the transmitter array spacing and receiver array spacing. Because the receiver antenna array is fixed to 8 elements, a 4×4 MIMO system is chosen to have an allowance to change the receiver array spacing. From figures 4-9 and 4-10, we can observe that

when the spacing of transmitter array and receiver array is unequal, the capacity may reach maximum. The reference [4] explains that the correlation of unequal antenna spacing is lower than equal antenna spacing. So lower correlation coefficient result in high capacity. Figures 4-11 and 4-12 illustrate the capacity versus Tx standard deviation for LOS and NLOS, respectively. The standard deviation of element spacing is expressed as $\sigma_{\Delta} = \left[\frac{1}{N} \sum_{i=1}^{N} \left(a_i - \overline{a} \right)^2 \right]^{\frac{1}{2}}$, where N is the number of antenna array; a_i is element array spacing.The measured results show that the MIMO capacity is optimized When the standard deviation of Tx element spacing is ranging from 1 λ to 1.5 λ.

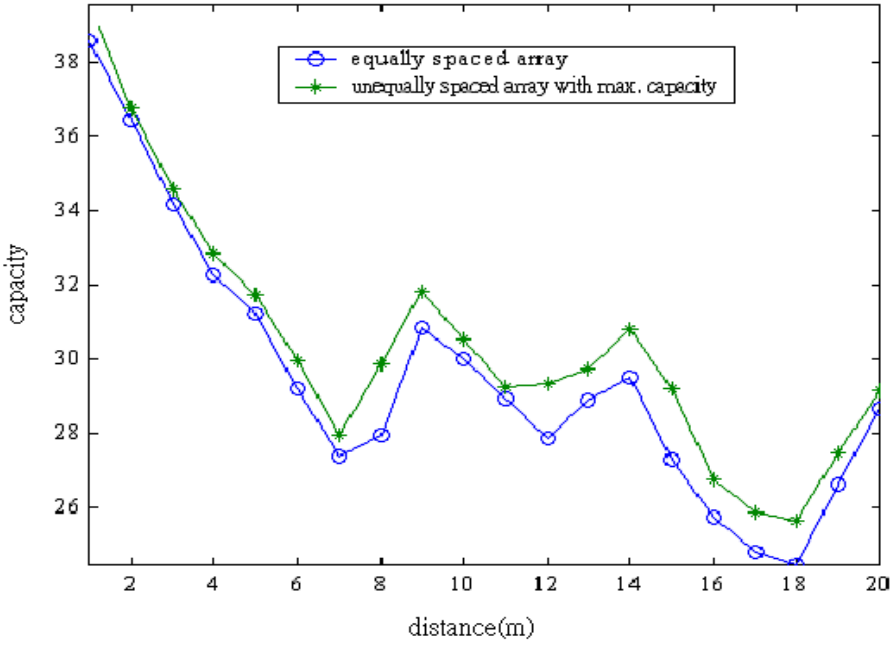

Figure 4-7 Capacity of equal antenna array and unequal antenna array as a function of d (Site A, path1)

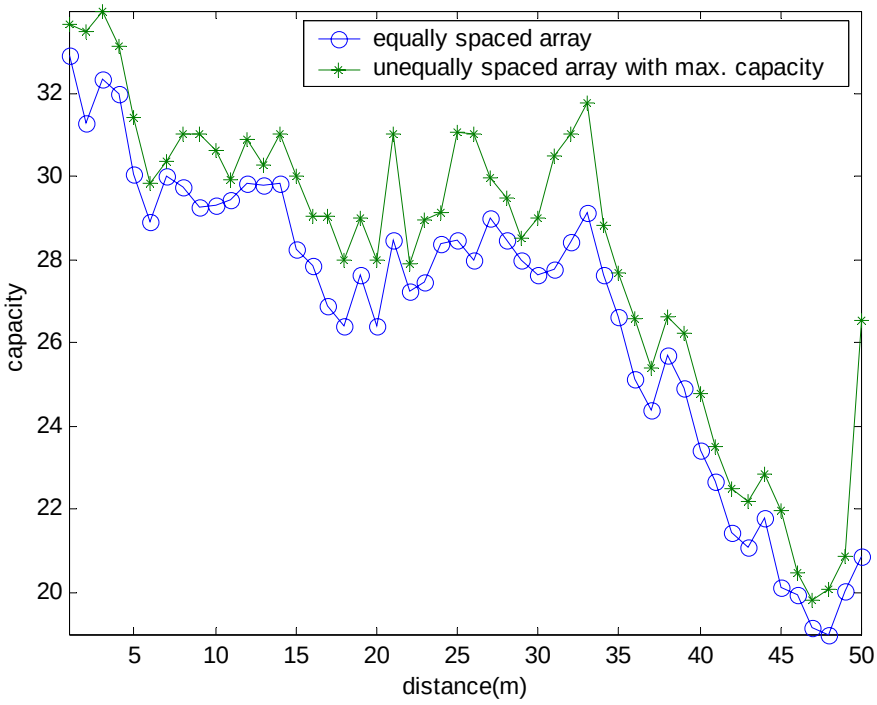

Figure 4-8 Capacity of equal antenna array and unequal antenna array as a function of d (Site A, path2)

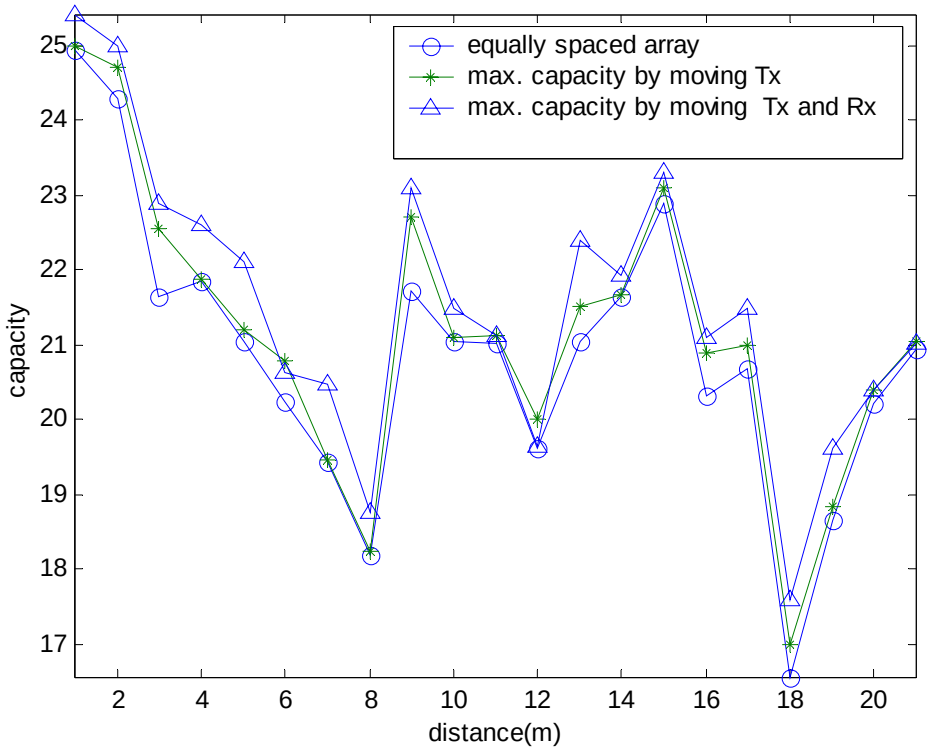

Figure 4-9 4x4 MIMO system capacity for equal array and unequal array (Site A,path1)

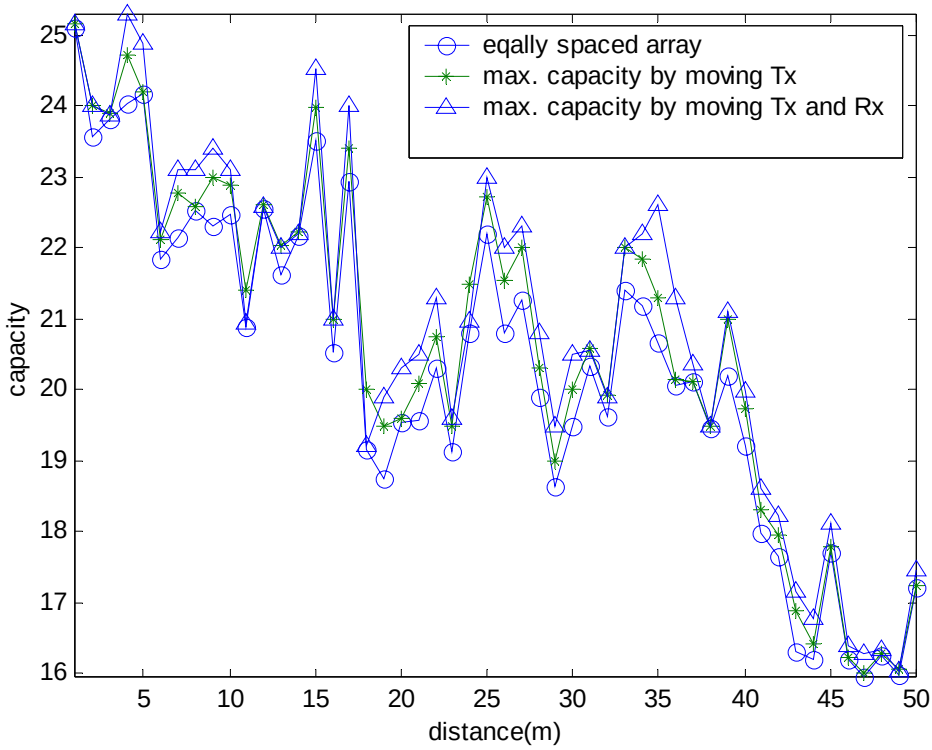

Figure 4-10 4x4 MIMO system capacity for equal array and unequal array (Site A,path2)

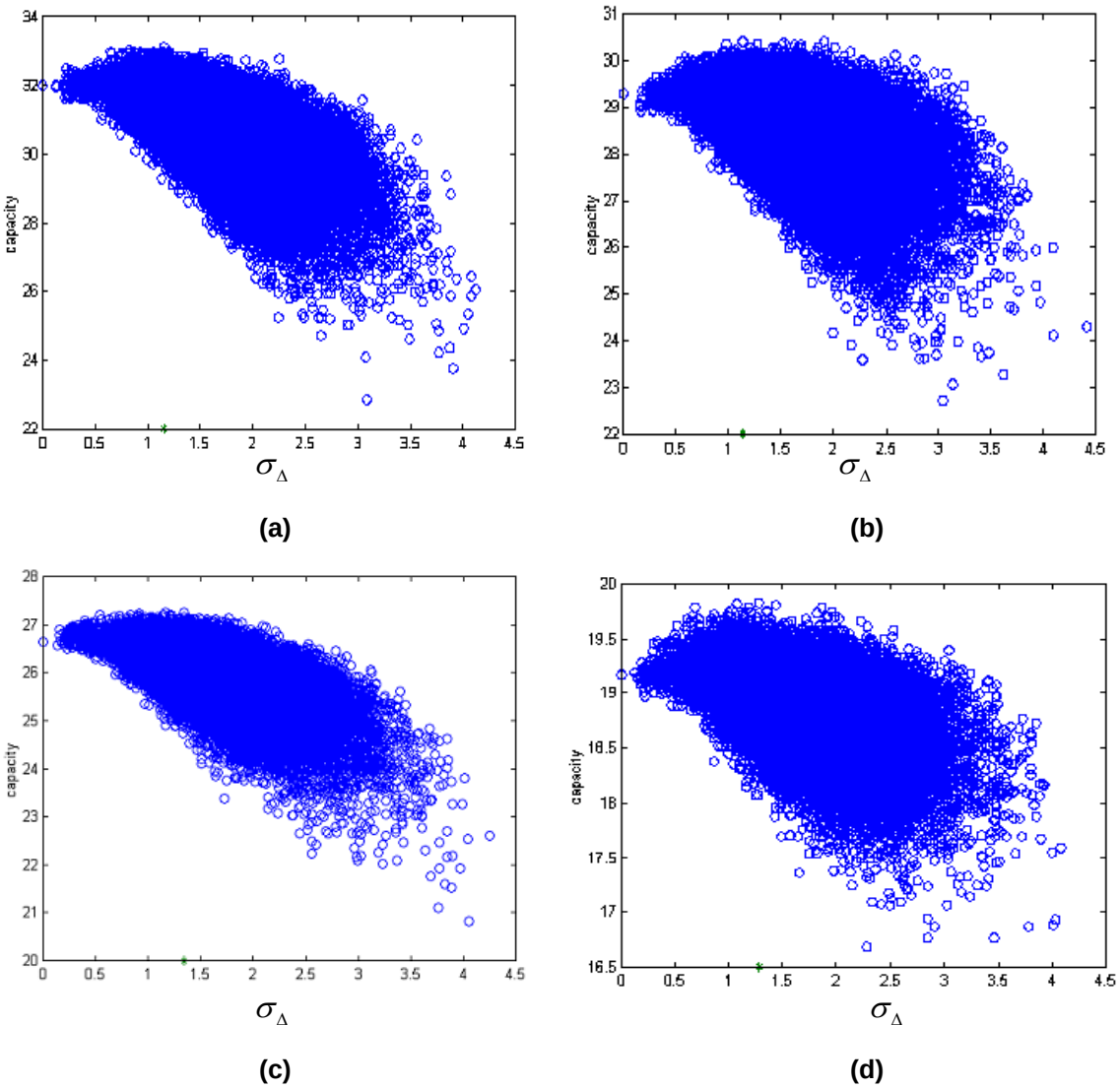

Figure 4-11 σ_Δ **for site A (LOS). In each figure, the maximum value of the capacity is located and its corresponding** σ_Δ **is shown as a mark *.**

(a) Tx-Rx distance: 4m (b) Tx-Rx distance:10m (c) Tx-Rx distance:15m (d) Tx-Rx distance: 20m

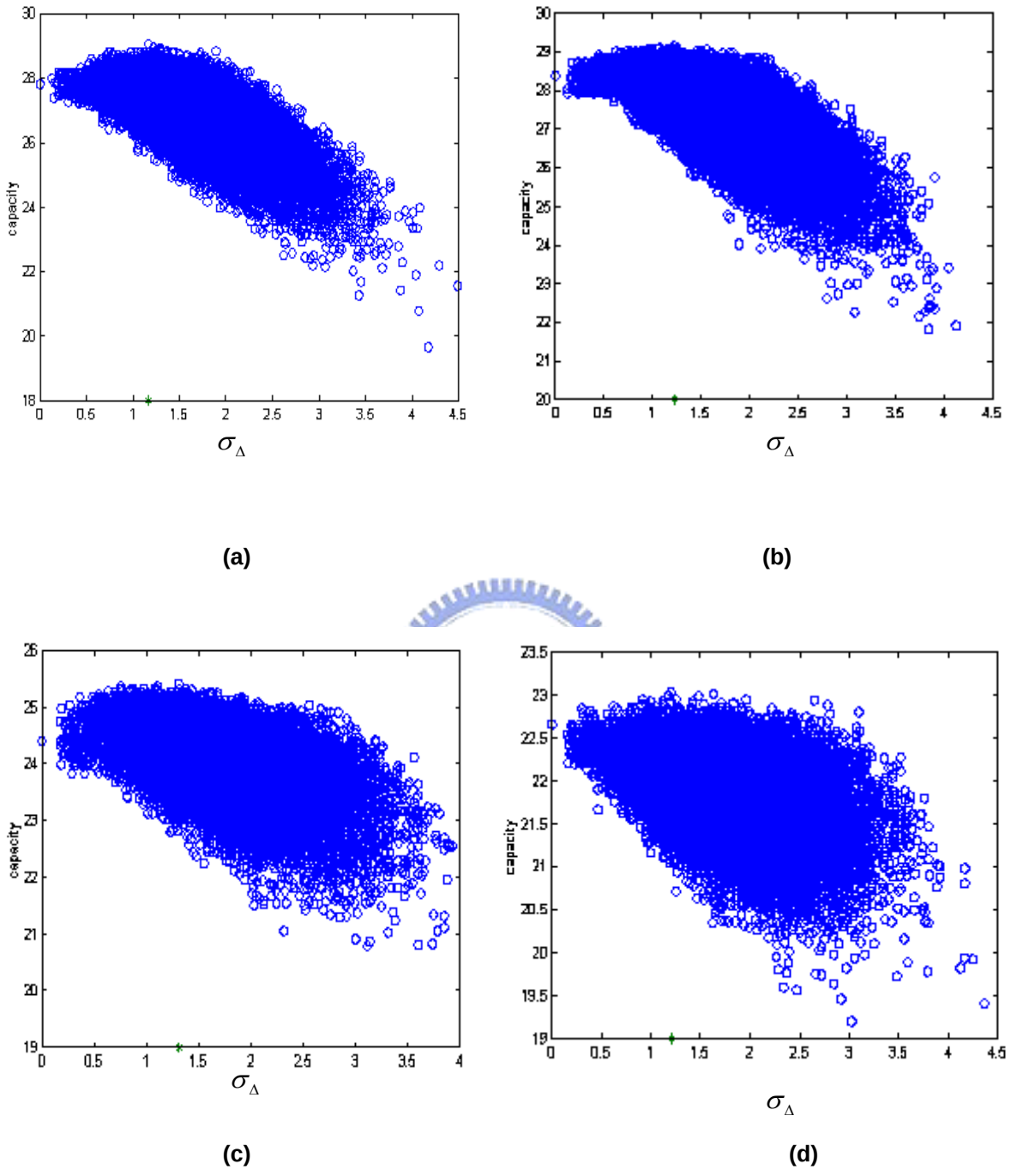

Figure 4-11 σ_Δ **for site A (LOS). In each figure, the maximum value of the capacity is located and its corresponding** σ_Δ **is shown as a mark *.**

(a)Tx-Rx distance: 16m (b) Tx-Rx distance:24m (c) Tx-Rx distance:37m

(d) Tx-Rx distance: 41m

4.3 Angle spread effect

To investigate the propagation environment effect on capacity and spatial correlations, we will introduce angle spread to observe the relation of capacity and propagation distance. The reference [12] mentions that for the large values of the angle spread will result in low correlation coefficient, low correlation coefficient obtains high capacity. We will observe the relation of capacity and angle spread during the measurement of site B, site C and site D.

At site B, the measurement carries out in the 2nd floor of the 4th Engineering Building. The measured path and Rx position illustrates in figure 3-3. From figure 4-13, it shows that capacity decreases along the hallway, but at the distance from 10m to 15m, we find that the capacity goes down suddenly. In order to explain this phenomenon, we can observe the measured map from figure 3-3, a lobby locates at the measured route from 10m to 15m and the lobby is an open area. We guess that in this open area, the angle spread decrease suddenly and the channel becomes correlated, so the capacity goes down suddenly. At figure 4-14, we plot the angle spread versus the propagation distance. We find that angle spread also decrease when the Tx-Rx distance increase. At 10m to 15m, angle spread also decrease suddenly. The measured result is as same as and reference [12], large angle spread may obtain more multipath. In multipath richness environment, the channel correlation will become lower and the capacity will be larger.

To prove the angle spread how affects the capacity. We carry out the same measurements at different floor. Site C and site D measured in 4th floor and 5th floor of the 4th Engineering Building, respectively. The measured route illustrate at figure 3-5 and figure 3-6. The 4th floor and 5th floor have the same structure, but in the 5th floor the wall is constructed of glass and the wall of 4th floor is made of concrete. We will observe the different material of wall how affects the capacity.

From figure 4-15 and figure 4-17, we find that capacity also decrease when propagation distance increase. But under the same antenna array spacing, the capacity of site C is always larger than the site D. We guess that the wall of concrete will reflect more multipath than glass and angle spread of site C will also be larger than site D. Figures 4-16 and 4-18 show angle spread versus propagation distance for different floors. We find that in figure 4-16, angle spread is significant lager than figure 4-18. So under rich multipath and lager angle spread environments between each transmitter and receiver antenna pair, MIMO wireless communications systems achieve significant capacity gains over conventional single antenna systems.

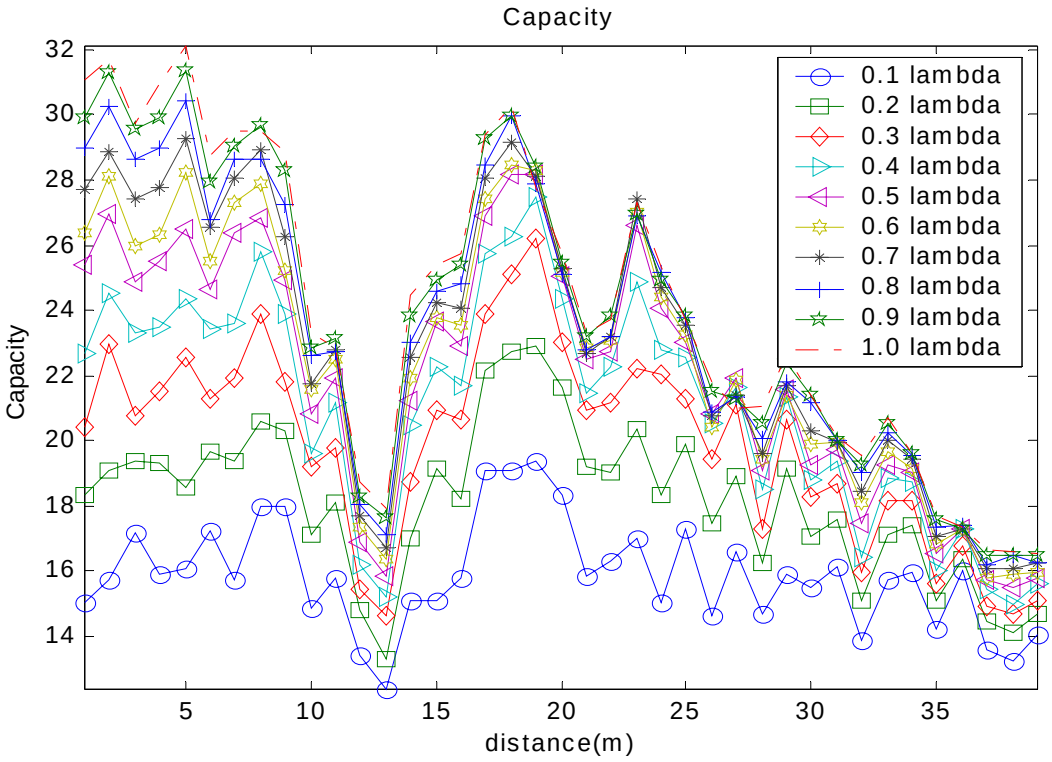

Figure 4-13 Capacity versus d for different Tx element spacing at Site B

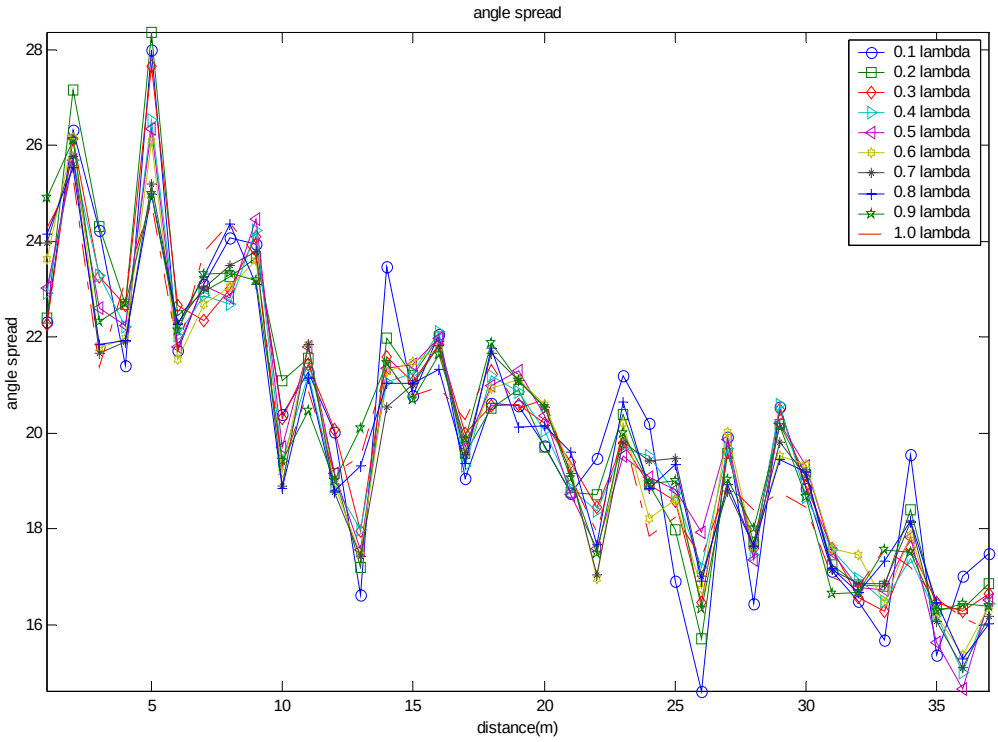

Figure 4-14 rms angle spread of AOA versus Tx-Rx distance at Site B

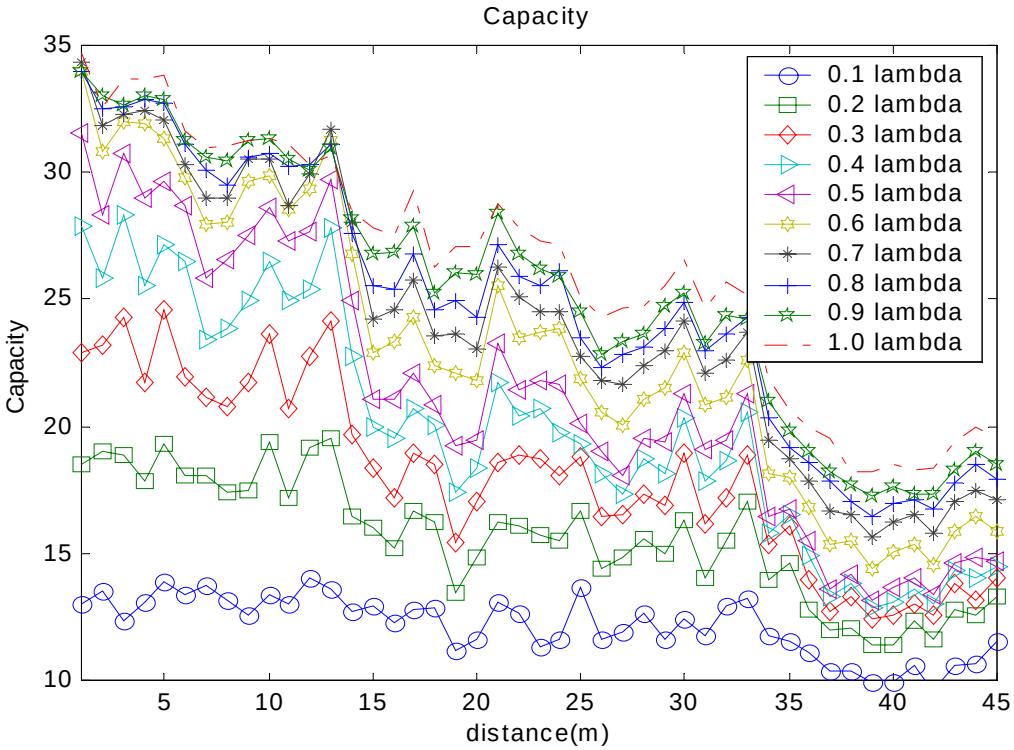

Figure 4-15 Capacity versus d for different Tx element spacing at Site C

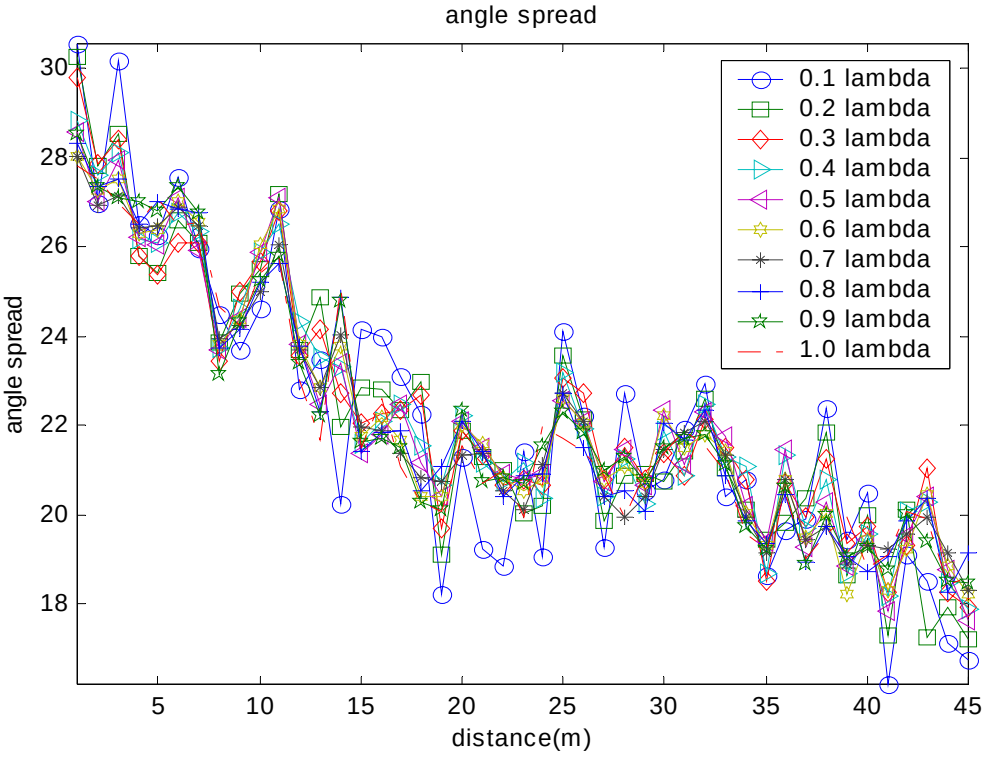

Figure 4-16 rms angle spread of AOA versus d at Site C

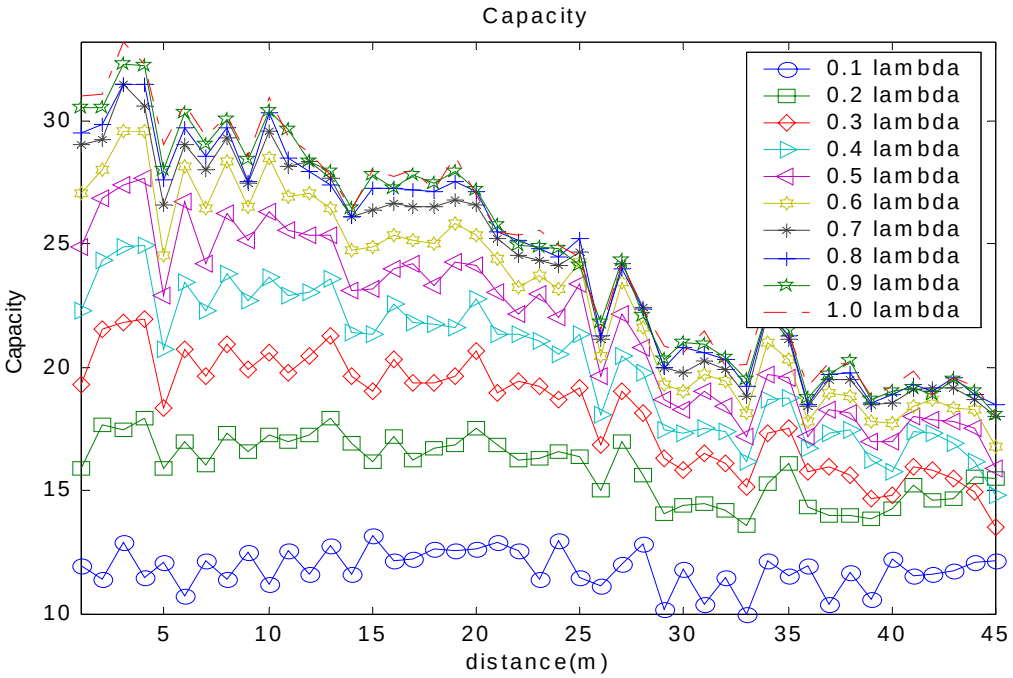

Figure 4-17 Capacity versus d at Site D for different Tx element spacing

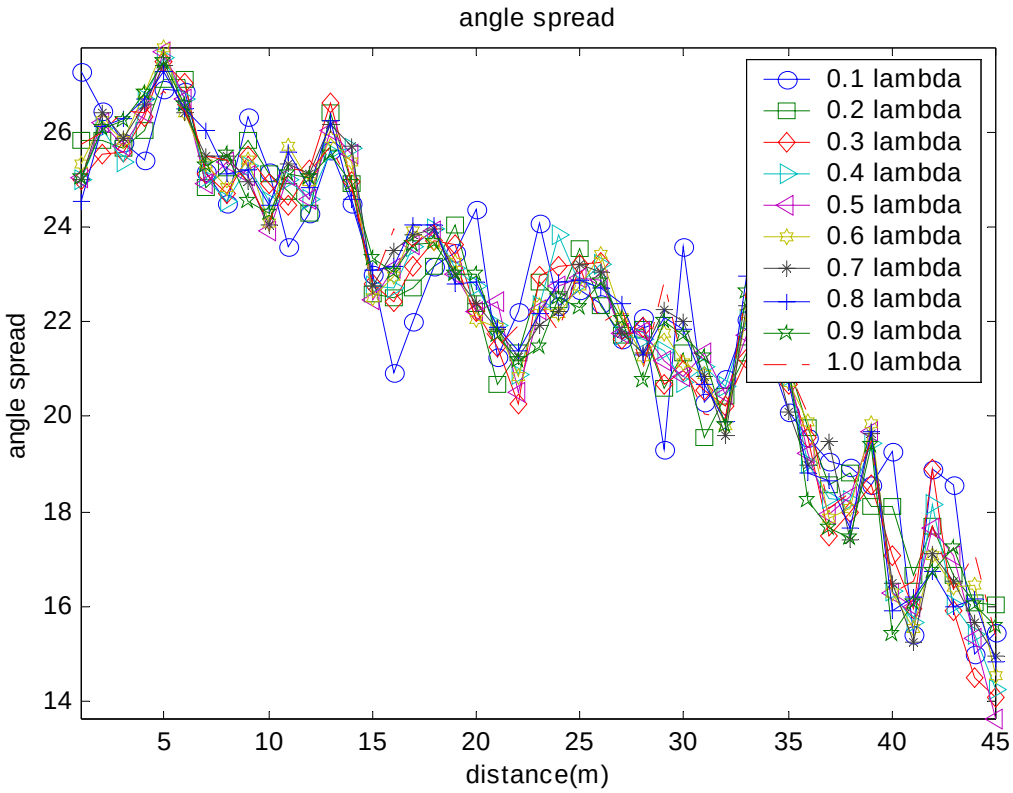

Figure 4-18 rms angle spread of AOA versus d at Site D for different Tx element spacing

4.4 Bandwidth effect

In this section, we investigate the impact of the signal bandwidth on the MIMO capacity. We choose 120M and 20M signal bandwidths to see how it affects the capacity. The experiment carried out in different floors (site C and site D). From figures 4-19 and 4-18, we can find that capacity of 120M-bandwidth is always greater than the 20M-bandwidth. Because the time resolution of 120M is 8.3ns and 20M is 49.8 ns, when bandwidth becomes large, time resolution decrease; hence array resolved more multipaths and channel becomes uncorrelated, uncorrelated channel results in high capacity.

Figures 4-21 and 4-23 illustrate multipath number versus distance; the result shows that multipath numbers of 120M-bandwidth is always greater than 20M-bandwidth; the measured results prove that high bandwidth will resolve more multipath numbers. According to section 4-3, angle spread is also in proportion to capacity. On different bandwidth, we also observe the variation of angle spread versus MIMO capacity. From figures 4-22 and 4-24, we find that on different bandwidth, the angle spread almost similar. So the capacity bases on different bandwidth, the main effect are multipath numbers, in multipath richness environment, the capacity will be higher.

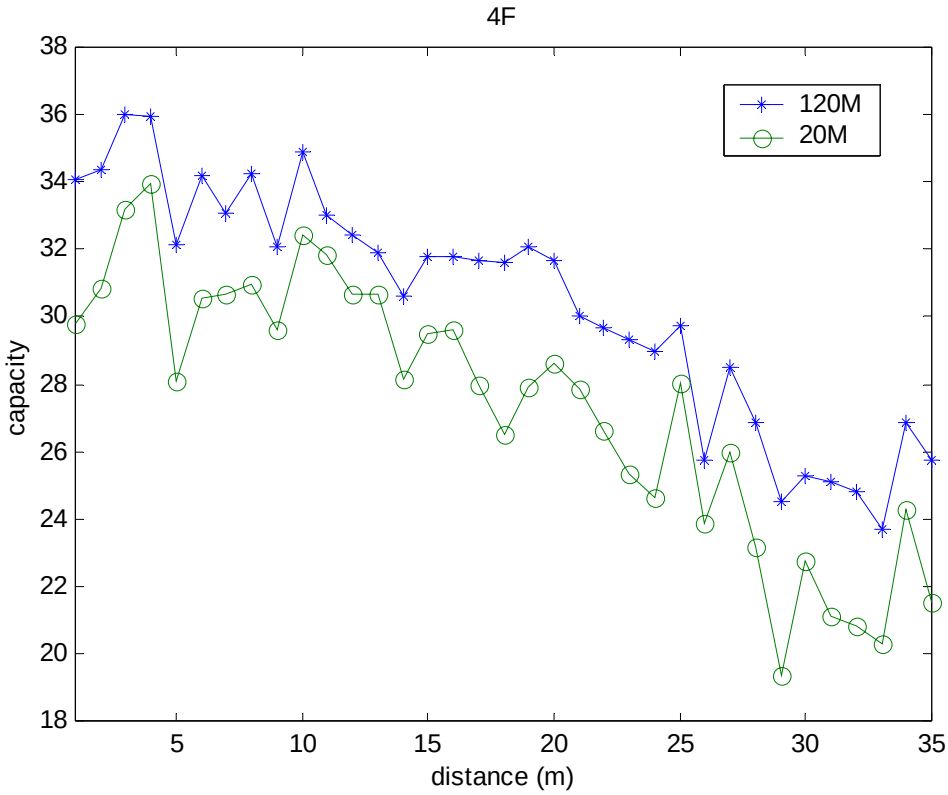

Figure 4-19 Capacity versus d at site C for signal bandwidths of 20MHz and 120MHz

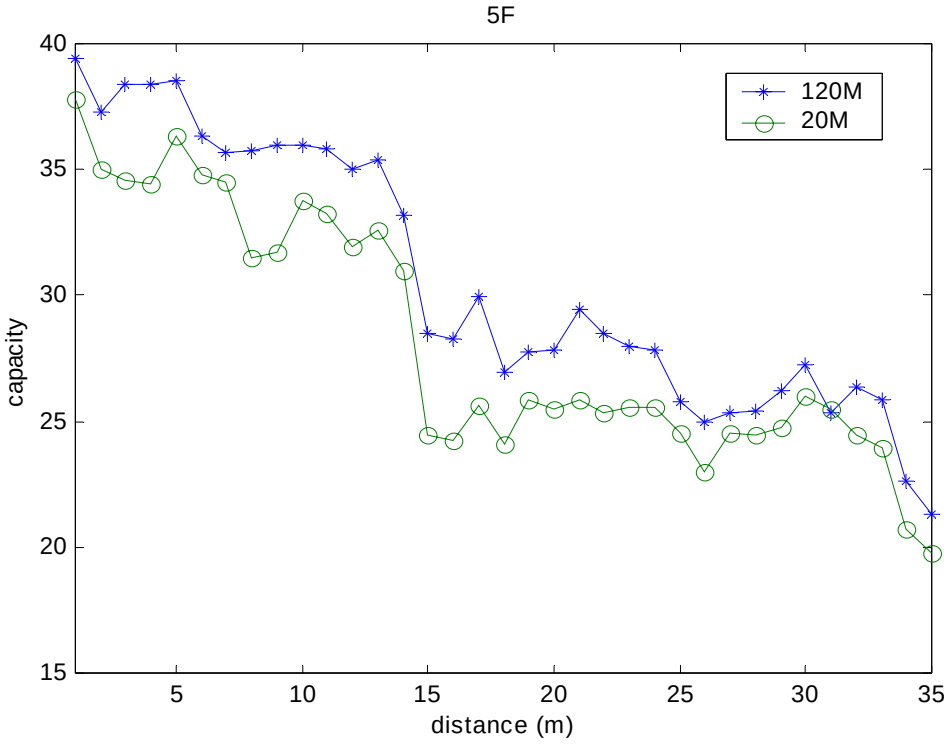

Figure 4-20 Capacity versus d at site D for signal bandwidths of 20MHz and 120MHz

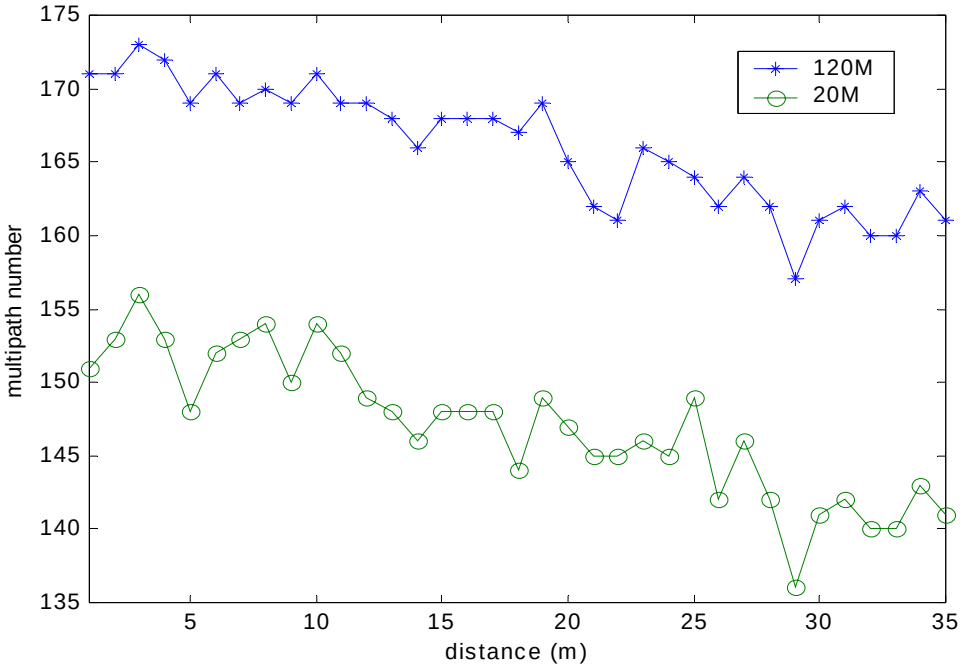

Figure 4-21 Number of multipath components at for signal bandwidths of 20MHz and 120MHz (site C)

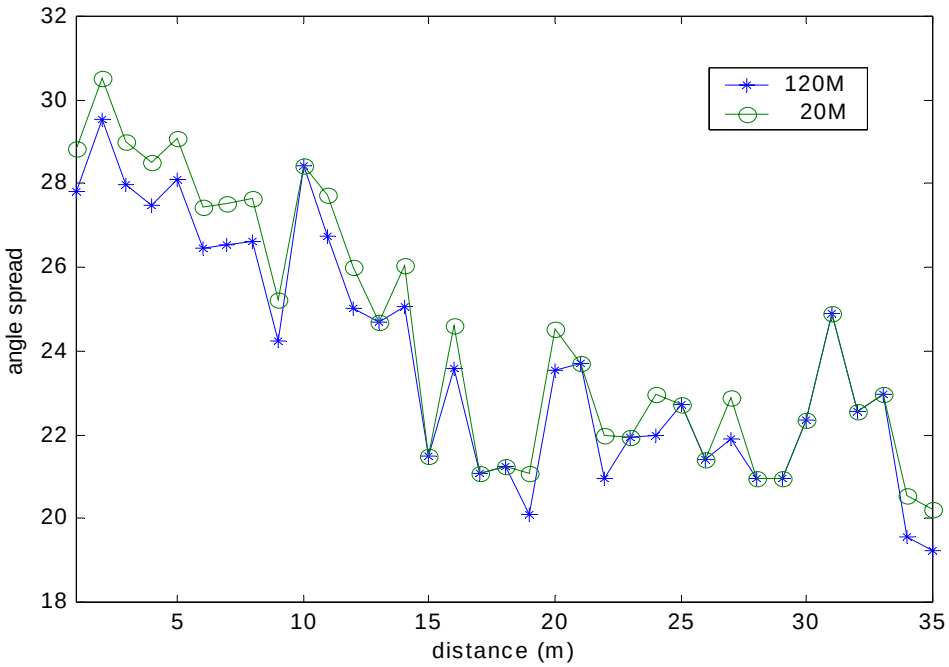

Figure 4-22 rms angle spread of AOA versus d for signal bandwidths of 20MHz and 120MHz (site C)

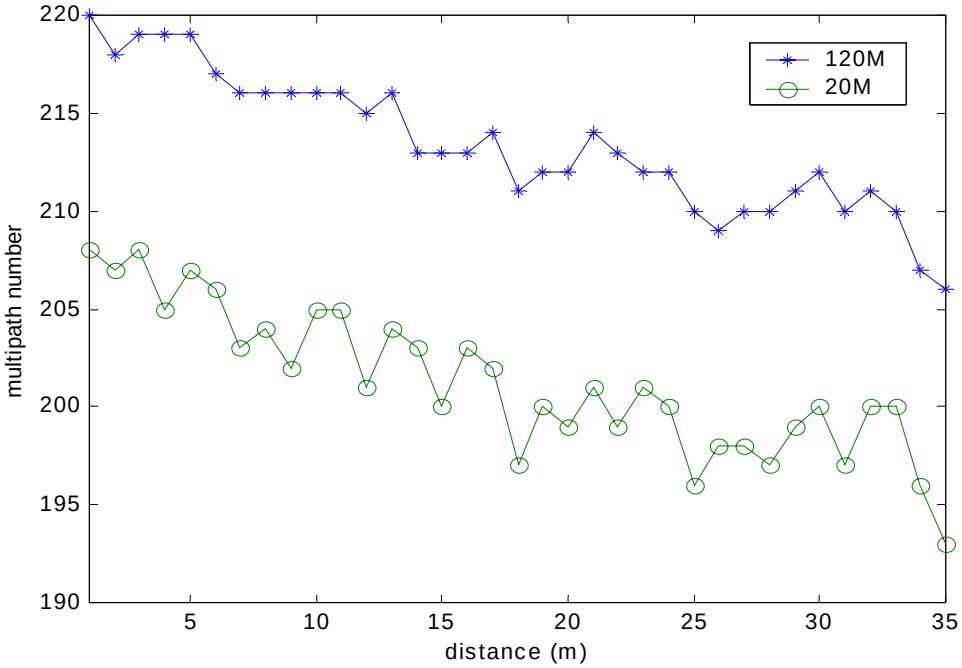

Figure 4-23 Number of multipath components at for signal bandwidths of 20MHz and 120MHz (site D)

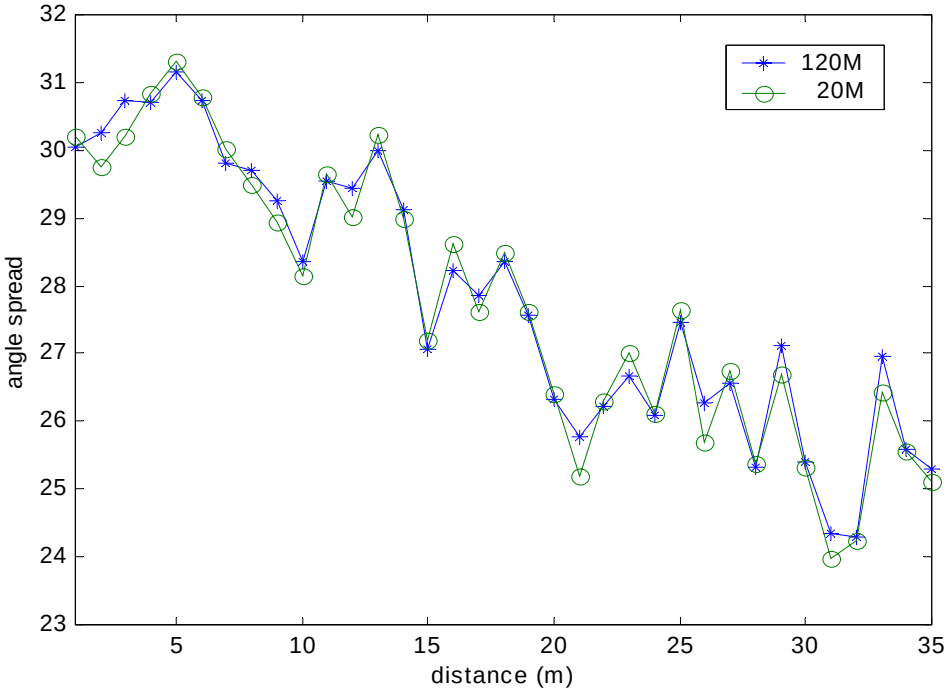

Figure 4-24 rms angle spread of AOA versus d for signal bandwidths of 20MHz and 120MHz (site D)

4.5 Local scatterer effect

In this section, we analyze the local scatterer how affects the MIMO capacity. The figure 4-25 descried the measured environments. We measured at each receiving 9 points for each room, the broadside direction of receiving linear array points at three individual directions with 120° interval. Therefore, 3 MIMO capacity values are shown for each point. Figure 4-25 illustrates that direction of receiving array is not significant effect on capacity. At figure 4-26, we place two scatterers at each room and observe the variation of capacity, it shows that when the receiving array is directional to scatterer, the capacity is significant higher than others direction, it is because the scatterer reflect more multipath , more multipath result in low correlation coefficient and obtain higher capacity. But from figure 4-26, we also find that scatterer only has significant effect on neighboring receiving array. At figure 4-27 we analyze how far the scatterer affects MIMO capacity. We measured at each receiving 12 points for each room, the broadside direction of receiving linear array point to scatterer. The interval distance of each receiver is 0.5m; figures 4-27 and 4-28 show MIMO capacity with scatterer and no scatterer condition, respectively. After comparing to measured results, we find that when the receiver within 1.5m from scatterer, MIMO capacity significant increases. In indoor environment, the effect distance of scatterer is about 1.5m.

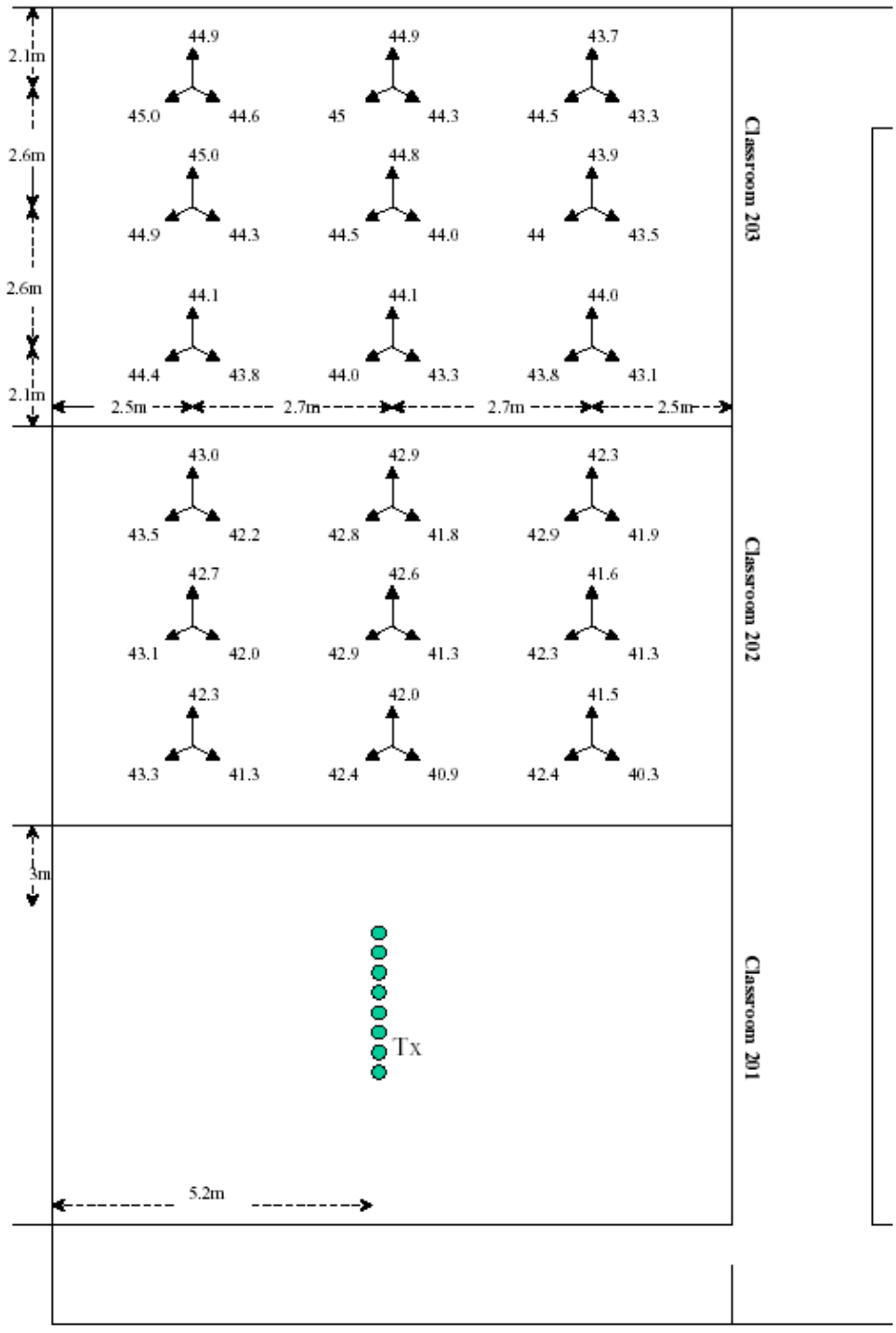

Figure 4-25 MIMO capacity measured at each receiving 9 points for each room, the broadside direction of receiving linear array points at three individual directions with 120 intervals. Therefore, 3 MIMO capacity values are shown for each point

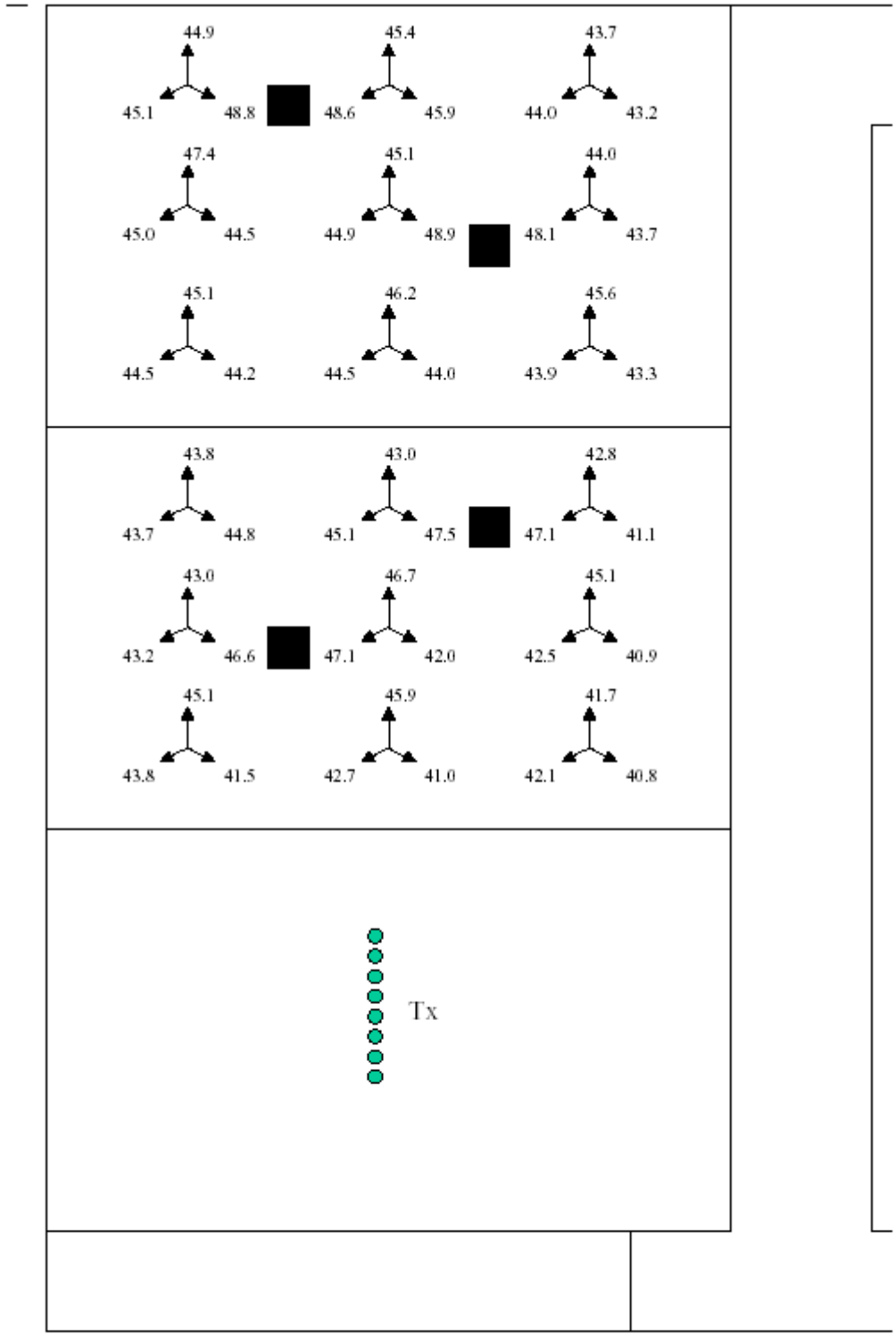

Figure 4-26 MIMO capacity measured at each receiving 9 points for each room with scatterers, the broadside direction of receiving linear array points at three individual directions with 120° interval. Therefore, 3 MIMO capacity values are shown for each point

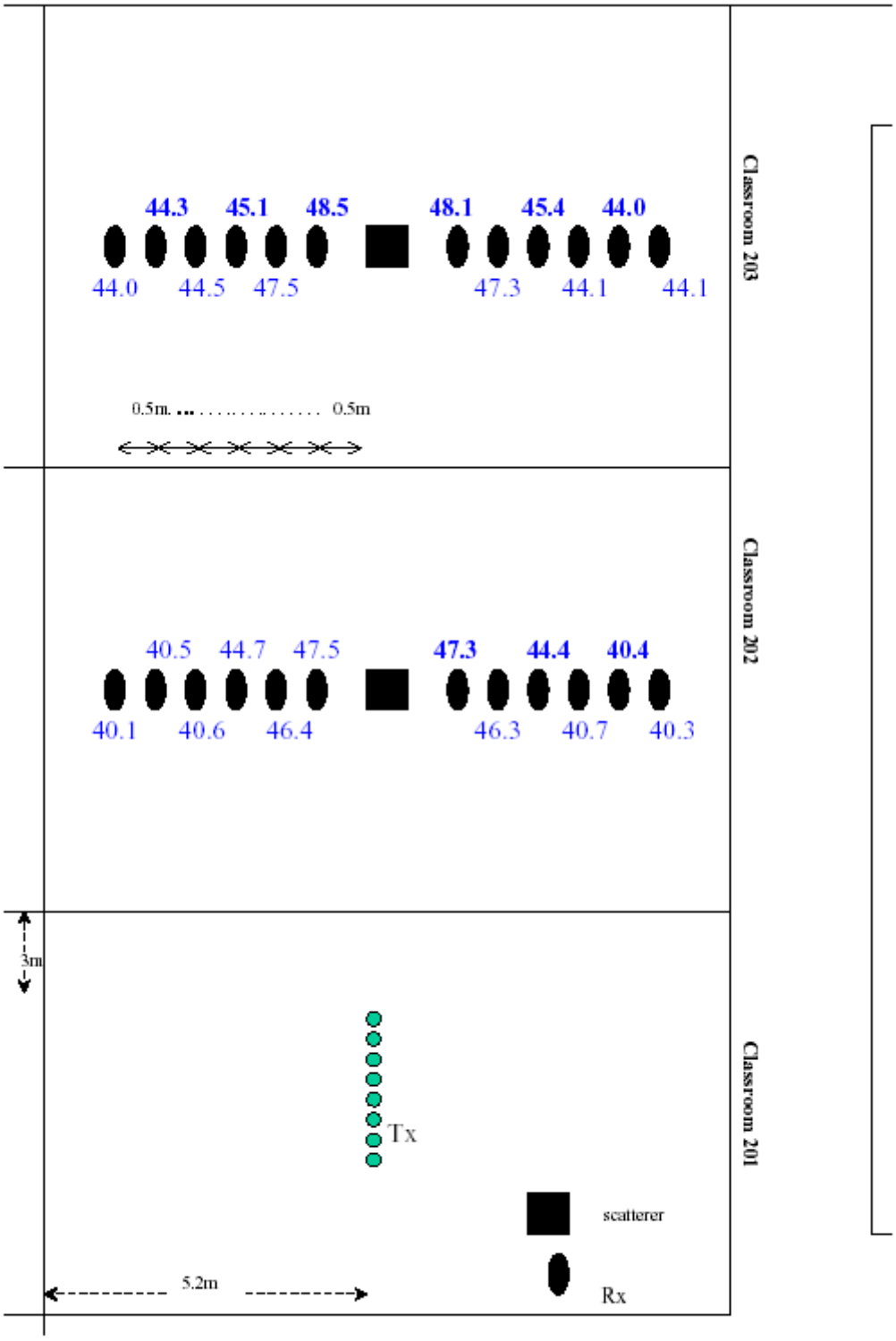

Figure 4-27 MIMO capacity measured at each receiving 12 points for each room, the broadside direction of receiving linear array point to scatterer.

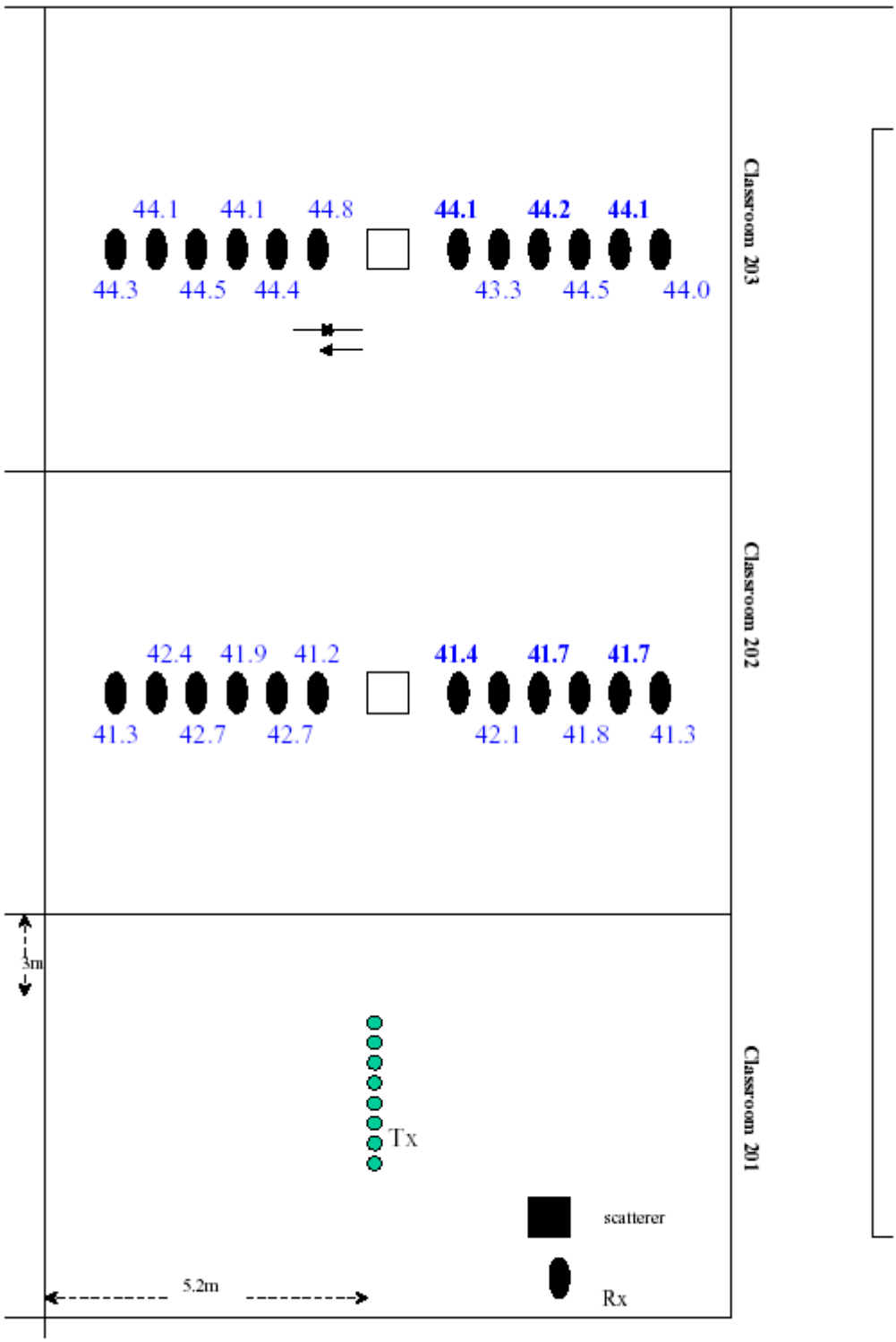

Figure 4-28 MIMO capacity measured at each receiving 12 points for each room (without scatterer)

Chapter 5

Conclusion

In this thesis the analysis of the impact of various conditions on 8x8 and 4x4 MIMO systems, capacity and correlations has been presented, including antenna spacing, angle spread, Tx-Rx distance, bandwidth and local scatter. The measurement using the RUSK channel sounder was carried out in the National Chiao Tung University campus. In this research, some phenomena are reveal and listed as following.

(1) Antenna array element spacing effect: antenna spacing may affect MIMO capacity and correlations significantly. The MIMO capacity increases as the element spacing increases and it saturates when the spacing is larger than one wavelength. This reveals that the correlation distance between the elements in indoor environments is about one wavelength. It is also found that when the standard deviation of Tx element spacing is ranging from 1 λ to 1.5 λ . The capacity of the MIMO with unequal array spacing is always larger than equal spacing. (2) Propagation distance effect: MIMO capacity is also decreased as the Tx-Rx distance increases for both LOS and NLOS cases. It is because that when the Tx-Rx distance decreases, the rms angle spread of AOA increases, which reduces the correlation between the Tx and Rx elements. (3) Bandwidth effect: MIMO capacity will increase as the signal bandwidth increases. It is because that signal bandwidth becomes larger so that time resolution smaller; hence the antenna array resolves more multipath components, channel which leads to lower correlation among spatial channels, i.e., is higher capacity. (4) Local scatterers effect: MIMO capacity increases due to transmitted signals disturbed by local scatterers so that the angle spread increases, large angle spread leads to high capacity. This

phenomenon can be observed at section 4.5. In indoor environments, when receiver is away from local scatterers about 1.5m, local scatter has no significant effects on MIMO capacity.

Some phenomena already shown in references [3], [4] and [5]. Our research demonstrates something new, we also found that (1) MIMO capacity saturates when the spacing is larger than one wavelength. (2) When the standard deviation of Tx element spacing is ranging from 1 λ to 1.5 λ. The capacity of the MIMO with unequal array spacing is always larger than equal spacing. (3) Reference [14] mentions that larger angle spread leads higher capacity, but not to proved it. Our research calculates the angle spread and proves the results. (4) It is also found that signal bandwidth has significant effects on MIMO capacity.

Reference

[1] Joseph C. Liberti, Jr.and Theodore S. Rappaport, “Smart Antennas for Wireless Communications: IS-95 and Third Generation CDMA Applications,” Prentice Hall, 1999

[2] G. J. Foschini and M. J. Gans, “On limits of Wireless Communications in a Fading Environment When Using Multiple Antennas,” Wireless Personal Communications, vol. 6, No. 3, pp. 311-335, March 1998

[3] Pohl, V.; Jungnickel, V.; Haustein, T.; von Helmolt, C., “Antenna Spacing in MIMO Indoor channels,” Vehicular Technology Conference, 2002. VTC Spring 2002, IEEE 55th, vol.2, pp. 749 –753, May 2002

[4] Jeng-Shiann Jiang; Ingram, M.A.; ”Enhancing measured MIMO capacity by adapting the locations of the antenna elements,” Personal, Indoor and Mobile Radio Communications, 2002. The 13th IEEE International Symposium on, vol.3, pp.1027 – 1031, Sept. 2002

[5] Kyritsi, P.; Cox, D.C, “Correlation Properties of MIMO Radio Channels for Indoor Scenarios,” Signals, Systems and Computers, 2001 Conference Record of the Thirty-Fifth Asilomar Conference on, vol. 2, pp. 994 –998, Nov. 2001

[6] Ivrlac, M.T.; Utschick, W.; Nossek, J.A.;” fading correlations in wireless MIMO,” IEEE Journal on Selected Areas in Communications, vol.21 , Issue: 5, pp:819 – 828, June 2003

[7] Wallace, J.W.; Jensen, M.A.;” Measured characteristics of the MIMO wireless channel,” Vehicular Technology Conference, 2001. VTC 2001 Fall. IEEE VTS 54th , Volume: 4 , pp.2038 – 2042, Oct. 2001

[8] Kermoal, J.P.; Schumacher, L.; Mogensen, P.E.; Pedersen, K.I.; “Experimental investigation of correlation properties of MIMO radio channels for indoor picocell scenarios,” Vehicular Technology Conference, 2000. IEEE VTS-Fall VTC 2000. 52nd, vo1, pp.14 – 21, Sept. 2000

[9] MDAV Corp.,”RUSK NTU/NCTU Training Section, 2001

[10] M. A. Beach, D. P. McNamara, P. N. Fletcher and P. Karlsson, “MIMO-A Solution for Advanced Wireless Access?,” 11th International Conference on Antennas and Propagation, pp. 231-235, April 2001

[11] Svantesson, T.; Wallace, J.;” On signal strength and multipath richness in multi-input multi-output systems,” Communications, 2003. ICC '03. IEEE International Conference on, vol.4, pp.2683 – 2687, May 2003

[12] Gesbert, D.; Bolcskei, H.; Gore, D.; Paulraj, A.;” MIMO wireless channels: capacity and performance prediction,” Global Telecommunications Conference, IEEE, vol.2, pp.1083 – 1088, Dec. 2000